PONTIFÍCIA UNIVERSIDADE CATÓLICA DE MINAS GERAIS
Programa de Pós-graduação em Odontologia

Carolina Drumond de Barros e Azevedo

DETERMINAÇÃO DA DOSE DE RADIAÇÃO E RISCO RADIOINDUZIDO EM EXAMES TOMOGRÁFICOS CONE BEAM PARA A AVALIAÇÃO DA ATM

Belo Horizonte
2016

Carolina Drumond de Barros e Azevedo

DETERMINAÇÃO DA DOSE DE RADIAÇÃO E RISCO RADIOINDUZIDO EM EXAMES TOMOGRÁFICOS CONE BEAM PARA A AVALIAÇÃO DA ATM

Dissertação apresentada ao Programa de Pós-graduação em Odontologia da Pontifícia Universidade Católica de Minas Gerais, como requisito parcial para obtenção do título de Mestre em Odontologia, Área de Concentração em Clínicas Odontológicas – Área Temática: Radiologia Odontológica e Imaginologia.
Linha de pesquisa: Métodos de Diagnóstico por Imagem, Radiobiologia e Radioproteção.

Orientador: Prof. Dr. Elton Gonçalves Zenóbio
Coorientador: Prof. Dra. Madelon Aparecida Fernandes Zenóbio

Belo Horizonte
2016

FICHA CATALOGRÁFICA
Elaborada pela Biblioteca da Pontifícia Universidade Católica de Minas Gerais

Azevedo, Carolina Drumond de Barros e
A994d Determinação da dose de radiação e risco radioinduzido em exames tomográficos Cone Beam para a avaliação da ATM / Carolina Drumond de Barros e Azevedo. Belo Horizonte, 2016.
103 f. : il.

Orientador: Elton Gonçalves Zenóbio
Coorientadora: Madelon Aparecida Fernandes Zenóbio
Dissertação (Mestrado) – Pontifícia Universidade Católica de Minas Gerais. Programa de Pós-Graduação em Odontologia.

1. Tomografia computadorizada de feixe cônico. 2. Radiação - Dosimetria. 3. Articulação temporomandibular - Radiografia. 4. Dosimetria termoluminescente. I. Zenóbio, Elton Gonçalves. II. Zenóbio, Madelon Aparecida Fernandes. III. Pontifícia Universidade Católica de Minas Gerais. Programa de Pós-Graduação em Odontologia. IV. Título.

CDU: 616.314-073

Carolina Drumond de Barros e Azevedo

DETERMINAÇÃO DA DOSE DE RADIAÇÃO E RISCO RADIOINDUZIDO EM EXAMES TOMOGRÁFICOS CONE BEAM PARA A AVALIAÇÃO DA ATM

Dissertação apresentada ao Programa de Pós-graduação em Odontologia da Pontifícia Universidade Católica de Minas Gerais, como requisito parcial para obtenção do título de Mestre em Odontologia. Área de Concentração: Clínicas Odontológicas – Área Temática: Radiologia Odontológica e Imaginologia.

COMPOSIÇÃO DA BANCA EXAMINADORA:

1- Profa. Dra. Maria do Socorro Nogueira – CDTN/CNEN
2- Prof. Dr. Flávio Ricardo Manzi – PUC Minas
3- Prof. Dr. Élton Gonçalves Zenóbio – PUC Minas

DATA DA APRESENTAÇÃO E DEFESA: 21 de dezembro de 2016

A dissertação, nesta identificada, foi aprovada pela Banca Examinadora

Belo Horizonte, 31 de janeiro de 2017

Prof. Dr. Élton Gonçalves Zenóbio
Orientador

Prof. Dr. Martinho Campolina Rebello Horta
Coordenador do Programa de Pós-graduação em Odontologia

AGRADECIMENTOS

Mais uma etapa da minha vida concluída com êxito. Agradeço nesse pequeno espaço, primeiramente a **Deus** por me guiar, iluminar e acolher.

A minha família toda, em especial aos meus pais, **Graça** e **Marcelo**, por terem compartilhado seus valores e saberes, pelo amor, apoio, confiança e investimento nas minhas escolhas;

Aos meus amigos **Alexandre Paim, Aloísio Araújo** e **Guilherme Martinez,** por serem os melhores amigos que alguém pode querer.

Ao namorado **Arthur Santos,** pelo incentivo, apoio, companheirismo e carinho. Sua paciência e conforto foram fundamentais.

A **todos meus colegas do mestrado** que me ajudaram a crescer como pessoa e foram fundamentais na minha formação profissional, em especial os colegas e amigos **Flávia Souza, Alexandre Greco, Aline Freitas, Sâmila Barra, Gabriel Ponte, Bárbara Niquini, Maria Isabel, Mariana Quinaud e Stéphanie Quadros** por me incentivarem a mostrar o melhor de mim, me acolherem quando precisei e por sempre proporcionarem momentos animados e inesquecíveis durante todo o programa.

Assim como os **queridos professores** que sempre estiveram dispostos a me direcionar, orientar e aconselhar, em especial o Prof. **Dr. Flávio Manzi** por sempre me escutar, nortear, acreditar no meu potencial, me incentivar a ser cada dia melhor para alcançar meus objetivos com sucesso, além de ser um excelente profissional que transmite em suas aulas o amor pela profissão, o que me motiva a seguir em frente.

Ao meu orientador **Prof. Dr. Elton Zenóbio**, minha coorientadora **Dra. Madelon Zenóbio** e à equipe do **CTDN/CNEN** por me incentivarem a buscar o melhor de mim e me ajudarem no projeto de pesquisa do mestrado com devoção, atenção e orientação.

Ao coordenador do Programa de Pós-Graduação da PUC Minas, Prof. Dr. **Martinho Campolina**, por sempre ajudar os alunos quando solicitado, além da seriedade e competência que o leva a ser exemplo de muitos alunos e profissionais.

A equipe da **Radius Odonto** por permitirem a realização dos exames na clínica.

Aos funcionários do Programa de Pós-Graduação da PUC Minas, em especial **Maria Angélica Paradizi** e **Silvania Martins**, por sempre estarem disponíveis a ajudar de maneira eficiente, profissional, e cordial, além do apoio que vocês transmitem aos alunos. Vocês foram fundamentais!

Esses dois anos se passaram como um piscar de olhos, ainda há muito chão pela frente. Obrigada a todos que fizeram parte do meu caminho. Vocês têm um lugar especial no meu coração e nas minhas lembranças.

“A menos que modifiquemos à nossa maneira de pensar, não seremos capazes de resolver os problemas causados pela forma como nos acostumamos a ver o mundo” (EINSTEIN).

RESUMO

Este estudo avaliou os valores de dose na superfície de entrada na pele, dose equivalente, dose efetiva, assim como o risco radioinduzido de câncer e alterações morfofuncionais, calculados de acordo com o BEIR VII (2006) nos órgãos e tecidos radiossensíveis. A avaliação total da articulação temporomandibular (ATM) foi realizada por meio da tomografia computadorizada de feixe cônico (TCFC) no tomógrafo *Kodak* 9000C 3D®, utilizando o protocolo de 4 aquisições tomográficas, sendo uma com o paciente de boca aberta e outra de boca fechada, de ambos os lados. Dosímetros termoluminescentes de Lif (TL-100H) foram posicionados em um simulador antropomórfico *Alderson RANDO*® do modelo feminino, em locais correspondentes: cérebro, cortical óssea, cristalino, glândulas salivares, mucosa oral, linfonodos cervicais, tireoide, esôfago, região extratorácica, medula óssea, pulmões, mamas, fígado, estomago, cólon, ovários, útero e bexiga. Os dosímetros foram analisados pela leitora *Harshaw 5500 Thermo Eléctron*® conectada a um computador com o *software Win-REMS*®. De acordo com os cálculos baseados no BEIR VII, os órgãos que apresentaram maiores riscos radioinduzido de câncer e alteração morfuncional são as glândulas salivares, cristalino e cérebro. As regiões das glândulas parótidas, cristalino e cérebro, obtiveram os maiores valores de dose equivalente durante o exame TCFC para avaliação da ATM, sendo 12,475mSv nas glândulas parótidas; 1,086mSv no cristalino; 0,753mSv no cérebro; As menores doses foram para as regiões abaixo da medula óssea (osso esterno) anatomicamente com valor de <0,007mSv. O valor da dose efetiva foi de 0,4709mSv. Os dados obtidos no presente estudo sugerem novas pesquisas para obtenção dos valores de dose em diferentes tomógrafos e medidas de proteção, além de estudos para a otimização da dose de radiação no exame de TCFC, com o intuito de reduzir ao mínimo possível a exposição à radiação durante o exame assim como a radiação secundária e a perda da qualidade de imagem.

Palavras-chave: Tomografia computadorizada de feixe cônico. Dosimetria. Articulação Temporomandibular. Dosimetria termoluminescente.

ABSTRACT

This study evaluated the values of entrance surface dose, equivalent dose, effective dose, as well as the risk of cancer and morphofunctional changes, calculated according to BEIR VII (2006) In radiosensitive organs and tissues. The total temporomandibular joint (TMJ) evaluation was performed using a conical beam computed tomography (CBCT) on the Kodak 9000C 3D® tomograph, using the protocol of 4 tomographic acquisitions, one with open mouth and one with closed mouth, on both sides. (TL-100H) were placed in an Alderson RANDO® anthropomorphic simulator of the female model, in corresponding places: brain, cortical bone, lens, salivary glands, oral mucosa, cervical lymph nodes, thyroid, esophagus, extrathoracic region, medulla Bone, lungs, breasts, liver, stomach, colon, ovaries, uterus and bladder. The dosimeters were analyzed by the Harshaw 5500 Thermo Electron® reader connected to a computer with Win-REMS® software. According to the calculations based on the BEIR VII, the organs that presented the greatest risk of cancer induced and morfunctional changes are the salivary glands, lens and brain. The regions of the parotid glands, lens and brain, obtained the highest equivalent dose values during the CBCT examination for TMJ evaluation, with 12,475mSv in the parotid glands; 1,086mSv in the lens; 0,753mSv in the brain; The lowest doses were for the regions below the bone marrow (sternal bone) anatomically with value of <0,007mSv. The effective dose value was 0,4709mSv. The data obtained in the present study suggest new research to obtain the dose values in different tomographs and protective measures, as well as studies for the optimization of the radiation dose in the CBCT examination, in order to minimize the exposure to radiation during the examination as well as secondary radiation and loss of image quality.

Keywords: Cone beam computed tomography. Dosimetry. Temporo-mandibular joint. Thermoluminescent dosimetry.

LISTA DE FIGURAS

LISTA DE QUADROS

LISTA DE TABELAS

LISTA DE ABREVIATURAS e SIGLAS

2D - Bidimencional
3D - Tridimencional
µGy - Micro Gray
µSv - Micro Sivert
ATM - Articulação temporomandibular
BEIR - *"Biologic Effects of Ionizing Radiation"* – Efeitos biológicos da radiação ionizante
CNEN - Comissão Nacional de Energia Nuclear
CDTN - Centro de Desenvolvimento da Tecnologia Nuclear
cm - Centímetros
D - Dose Absorvida
ESD - Dose da superfície de entrada
ECC - Fator de sensibilidade individual do dosímetro
FOV - *"Field of View"* - Campo de visão
Gy - Gray
ICRP - "*Internation commission the radiological protection*"
keV - Quilo elétrons-volt
kV - Quilovolts
kHz - Quilohertz
Kg - Quilograma
m - Metro
mA - Miliamperagem
MeV - Mega elétrons-volt
mGy - Miligray
mm - Milímetros
mg - Miligramas
mSv - Milisivert
nC - Nanoculombs
RCF - *Reader Calibration Factor* - Fator de calibração da leitora
RM - Ressonância magnética
TC - Tomografia computadorizada
TCFC - Tomografia computadorizada de feixe cônico
TCMS - Tomografia computadorizada MultiSlice
TL - Termoluminescente
SI - Sistema Internacional
Sv - Sivert

SUMÁRIO

1 INTRODUÇÃO

A articulação temporomandibular (ATM), é do tipo sinovial móvel composta, sendo classificada como a articulação mais complexa do corpo humano. Suas funções mais importantes são a mastigação e a fonação, sua avaliação possui grande interesse na área da odontologia (ALOMAR et al., 2007). A ATM pode ser acometida pelas mesmas condições patologias e desordens que afetam as demais articulações do organismo, merecendo uma atenção especial dos profissionais dessa área e realizações de exames por imagem para avaliações (RAMOS et al., 2004).

O método radiográfico convencional, utilizado para a avaliação das alterações ósseas da ATM é a radiografia transcraniana. Porém, este representa uma projeção bidimensional (2D) de estruturas tridimensionais (3D), sendo necessário, muitas vezes, obter mais de uma aquisição radiográfica, em outro plano, para melhor avaliação da região, devido as sobreposições de imagens da região. Com a introdução da tomografia computadorizada (TC), os componentes ósseos da ATM podem ser visualizados tridimensionalmente, quase totalmente livres de sobreposições. Sendo assim, atualmente este é o exame por imagem padrão-ouro para avaliação óssea da ATM, assim como a ressonância magnética (RM) é para os componentes moles desta articulação (ZHANG et al., 2013; KUMAR et al., 2015).

A tomografia computadorizada de feixe cônico (TCFC) foi desenvolvida na década de 90 dedicada para região dentomaxilofacial e apresenta imagens tridimensionais do tecido duro com maior resolução espacial, quase totalmente livres de sobreposições, assim como, menor dose de radiação ao paciente e fácil acesso da população quando comparado com a tomografia computadorizada multislice (TCMS) (SCARF; FARMAN; SUKOVIC, 2006; GARIB et al., 2007; ZHANG et al., 2013). É um exame por imagem radiográfica, cujo aparelho emite um feixe de raios X em forma de cone, centralizado em um detector da imagem. O conjunto fonte-detector realiza uma rotação, parcial ou de 360º, em torno do paciente, que deve estar estático, obtendo uma aquisição volumétrica das estruturas ósseas (FELDKAMP; DAVIS; KRESS, 1984; SCARFE; FARMAN, 2008). Esta técnica de imagem tem se tornado cada vez mais frequente no mercado odontológico, com tecnologias cada vez mais avançadas (VOS; CASSELMAN; SWENNEN, 2009; ZHANG et al., 2013).

A TCFC apresenta novos desafios no conhecimento das doses de radiação e proteção radiológica devido ao risco radioinduzido de câncer e alterações morfofuncionais aos órgãos e tecidos em pessoas expostas à radiação (INTERNATIONAL COMMISSION THE RADIOLOGICAL PROTECTION, 1991; NATIONAL RESEARCH COUNCIL, 2006; INTERNATIONAL COMMISSION THE RADIOLOGICAL PROTECTION, 2007; EUROPEAN COMMISSION, 2012). Os princípios de proteção radiológica, a justificação, a otimização e a limitação de doses, devem ser aplicados às práticas que envolvem a TCFC, observando-se que o seu uso se estende a área de clínicas odontológicas, otorrinolaringológicas e ortopédicas policlínicas que no passado não eram tipicamente associadas à TC (EUROPEAN COMMISSION, 2012).

O risco radioinduzido de câncer em TCFC, em exames craniofaciais, pode ser estimado por meio da avaliação da dose equivalente (mSv), dose efetiva (mSv) em órgãos radiossensíveis calculadas por meio de modelos computacionais e de dosímetros termoluminescentes posicionados em simuladores antropomórficos nas regiões dos órgãos radiossensíveis, como nos estudos dosimétricos realizados por Ludlow et al. (2006), Ludlow e Ivanovic (2008), Chau e Fung (2009), Zenóbio et al. (2012), Pauwels et al. (2012) e Morant (2013), Soares et al. (2015).

Ao realizar exames de imagem para diagnóstico, é essencial que o benefício para o paciente seja maior que o risco de exposição à radiação ionizante, que deve ter dose a mais baixa possível, porém sem perder a qualidade e nitidez da imagem. Desta forma, no presente estudo foram avaliadas as doses de radiação em exames TCFC para ATM, analisando a influência de risco radioinduzido nos órgãos com maior susceptibilidade a alterações morfológicas.

2 OBJETIVOS

2.1 Objetivo geral

Avaliar e calcular os valores de dose absorvida e dose na superfície de entrada, em exames de tomografia computadorizada feixe cônico realizados no tomógrafo *Kodak* 9000C 3D para avaliação da ATM utilizando o fantoma antropomórfico *Alderson-RANDO*, modelo feminino e detectores termoluminescentes (TL-100H).

2.2 Objetivos específicos

a) medição da dose na superfície de entrada (ESD) da região do cristalino, glândulas salivares, mucosa oral, linfonodos cervicais, tireoide e região extratorácica, mamas, fígado, estomago, cólon e bexiga;
b) medição da dose absorvida (D) na região do cérebro, medula óssea, cortical óssea, cristalino, glândulas salivares, mucosa oral, linfonodos cervicais, tireoide, esôfago, região extratorácica, pulmões, mamas, fígado, estômago, cólon, ovários, útero e bexiga;
c) avaliação e comparação dos valores de dose na superfície de entrada (ESD) e dose absorvida (D) nos pontos anatômicos avaliados;
d) cálculo da dose equivalente e dose efetiva de acordo com a ICRP 103 (2007), e risco radioinduzido de câncer e alterações morfofuncionais nos pontos anatômicos avaliados segundo os relatos do BEIR VII (2006).

3 MATERAL E MÉTODOS

O estudo realizado foi quantitativo analítico laboratorial experimental, utilizando a infraestrutura e apoio: dos laboratórios do Centro de Desenvolvimento de Tecnologia Nuclear (CDTN/CNEN):

a) Laboratórios de calibração: Irradiadores gama e raios X;
b) Laboratório de dosimetria termoluminescente:
   - ✓ detectores termoluminescentes 100H tipo pastilha, forno automático, leitora termoluminescente.

Do Serviço de Imagem e Diagnóstico Radius de Belo Horizonte:

a) Sala de exames: Tomógrafo computadorizado de feixe cônico *Kodak* 9000C 3D.

3.1 Apresentação dos materiais

Para realização desse estudo, foi necessário a utilização de 95 detectores termoluminescentes de LiF (TL-100H), simulador antropomórfico (*Alderson RANDO*), tomógrafo computadorizado de feixe cônico (*Kodak* 9000C 3D), irradiador gama STS, modelo OB85, forno automático (*Forno PTW modelo Freiburg*), Leitora *Harshaw* 5500 *Termo Eléctron* e *software Win-REMS*, desenvolvido pela *RPM-Bicron*, apresentados detalhadamente abaixo.

3.1.1 Detectores termoluminecentes de LiF:Mg,Cu,P:(TL-100H)

Os detectores termoluminescentes (TL) utilizados são do tipo pastilha e possuem dimensões 3mm x 3mm x 1mm, cerca de 24mg, fabricado *pela Harshaw-Bicron* (Figura 1). É constituído por fluoreto de lítio e dopado de impurezas magnésio, cobre e fósforo. Esses necessitam ser caracterizados antes de serem utilizados no simulador antropomórfico (HARSHAW-BICRON, 1998).

Figura 1: Detectores termoluminescentes (TL) de LiF:Mg,Cu,P(TL- 100H)

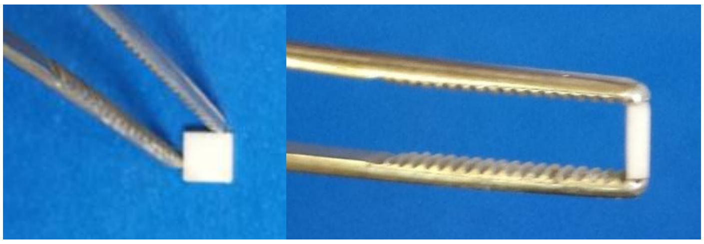

Fonte: Elaborado pela autora

3.1.2 Leitora Harshaw 5500 Thermo Eléctron

A leitura dos detectores TL foi realizada na leitora *Harshaw* 5500 *Thermo Eléctron* (Figura 2), conectada a um computador com o *software Win-REMS* (*Radiation Evaluation and Management System*) desenvolvido pela *RPM-Bicron* (THERMO ELECTRON CORPORATION, 2002).

Figura 2: Leitora Harshaw 5500 Thermo Eléctron

Fonte: **Elaborado pela autora**

3.1.3 Simulador antropomórfico Alderson-Rando

Desenvolvido pelo físico Ph.D. Lawrence H. Lanzl e fabricado pela *Alderson Research Laboratories*, é utilizado para avaliações relacionados a radiações em diversas áreas de pesquisa.

Sua constituição é de um material com a radiodensidade semelhante aos tecidos humanos, distribuído randomicamente (MATSUSHIMA, 2015).

O fantoma é dividido por 33 fatias, sendo que cada fatia contém uma matriz regular de furos, com diâmetro de 5mm cada, e espaçados em 3cm. Os furos contém cilíndros que servem como tampões e também para encaixar os detectores, com intuito de auxiliar na pesquisa na mensuração da radiação absorvida nos locais selecionados, por exemplo (CHAU; FUNG, 2009).

No presente estudo, foi utilizado o simulador antropomórfico *Alderson RANDO* no modelo feminino, representando uma mulher adulta padrão, com dimensões aproximadas de 1,55m de altura, massa de 50kg, mama correspondentes a mamas de 600mL e não apresenta braços e pernas (Figura 3), pertencente ao laboratório de radioproteção aplicado a mamografia (LARAM), do CDTN/CNEM de Belo Horizonte-MG.

Figura 3: Simulador antropomórfico - *Alderson-RANDO* feminino

Fonte: **Elaborado pela autora**

3.1.4 Tomógrafo Kodak 9000C 3D

O equipamento utilizado para o exame tomográfico de feixe cônico para avaliação da ATM no fantoma *Alderson-RANDO*, foi o *Kodak* 9000C 3D (Figura 4), pertencente ao Serviço de Imagem e Diagnóstico Radius de Belo Horizonte. As informações das especificações técnicas do equipamento utilizado estão demonstrados no Quadro 1.

Quadro 1: Especificações técnicas do Kodak 9000C 3D

Especificações técnicas- Kodak 9000C 3D	
Tensão do tubo	60- 90 kV
Corrente do tubo	2-15 mA
Frequência	140 kHz
Ponto focal do tubo	0,5mm
Filtração total	> 2,5mm Alumínio
Tamanho do Volume	50 x 37mm
Tamanho do Voxel isotrópico	76x76x76µm
Colimação (FOV)	5,0cm x 3,7cm

Fonte: **Elaborado pela autora**

Figura 4: Tomógrafo de feixe cônico Kodak 9000C 3D

Fonte: **Elaborado pela autora**

3.2 Metodologia

3.2.1 Etapa laboratorial

Os detectores TL foram selecionados observando critérios físicos (fratura, irregularidade, alteração de coloração), homogeneidade, reprodutibilidade e limite inferior de detecção de acordo com os requisitos estabelecidos pela ISO 12794 (INTERNATIONAL STANDARD NUCLEAR ENERGY, 2000), adotado no laboratório de dosimetria termoluminescente.

3.2.1.1 Sistema de leitura TL

A leitora TL *Harshaw*, modelo 5500, acoplada a um computador e ao *software Win-REMS*^{TM}, desenvolvido pela *RPM-Bicron*, contém uma série de programas e base de dados que direciona a operação da leitora. Esta foi ligada durante 20 minutos antes do início das leituras para estabilização e redução do ruído eletrônico. O perfil de tempo e temperatura são definidos no programa de acordo com o TL utilizado, sendo do presente estudo o TL LiF:Mg,Cu,P (TL-100H) com tempera de 240°C, tempo de 20 segundos e taxa de 120°C/segundo. Com isso, ele promove 3 etapas para cada TL e assim, realizar a leitura: Pré- aquecimento: estabelece o ponto para início da leitura comum a todos os detectores; Aquisição de dados: etapa em que os dados são adquiridos e a curva de emissão (“glow curve”) é gerada; Recozimento: aquece os detectores a uma alta temperatura para eliminação dos sinais residuais (THERMO ELECTRON CORPORATION, 2002).

3.2.1.2 Geração dos detectores de calibração

A etapa tem como objetivo selecionar o grupo de detectores que são utilizados no procedimento de calibração da leitora. Os detectores TL foram caracterizados utilizando uma fonte de ^{137}Cs do irradiador Gama STS *Steureurngstechknik & Strahlenschutz G-* modelo OB, do Laboratório de Calibração de Dosímetros do CDTN. Os detectores TL foram irradiados cinco vezes com 5 mGy de Kerma no ar com uma distância de 1,5m da fonte, em condições de equilíbrio eletrônico. Foram selecionados um grupo de 4 detectores com variação máxima da homogeneidade de 10% e reprodutibilidade de 7,5% em relação à média. (THERMO ELECTRON CORPORATION, 2002).

3.2.1.3 Calibração da leitora (obtenção do RCF)

A calibração da leitora é feita com o objetivo de obter o fator de calibração da leitora (RCF), e assim, converter o sinal da fotomultiplicadora, que é dado na unidade de carga (nC), para a unidade dosimétrica definida, dose absorvida e dose da superfície de entrada (mGy) (HARSHAW-BICRON, 2005).

Neste procedimento, 4 detectores selecionados para a calibração foram expostos a 5mGy de Kerma no ar pela fonte de ^{137}Cs do irradiador Gama *STS Steuerungstechnik & Strahlenschutz Gmbh*, modelo OB85 (Laboratório de Calibração de Dosímetros do CDTN), a uma distância de 1,5m em condições de equilíbrio eletrônico

Após a exposição, a calibração da leitora foi realizada utilizando-se a relação entre o valor do kerma no ar, em que os detectores foram expostos em mGy e o valor que a leitora fornece em nC. Assim, no próprio software definimos o fator de calibração da leitora, RCF (*Reader Calibration Factor*) como 0,0754 nC/µGy (THERMO ELECTRON CORPORATION, 2002).

3.2.1.4 Calibração individual dos detectores (obtenção do ECC)

Esse procedimento gera o fator de sensibilidade individual (ECC) para que todos os detectores obtenham semelhante resposta à dose de radiação aplicada, evitando uma variação natural referente à resposta do material e à massa física de fabricação, sendo assim pré-estabelecido no *software*, a seleção daqueles que estão em até 30% de diferença da resposta média do grupo de detectores

A calibração individual dos detectores proporciona uma redução da incerteza do procedimento da leitura, que devem apresentar o mesmo valor para uma determinada exposição à radiação. (THERMO ELECTRON CORPORATION, 2002).

3.2.1.5 Tratamento térmico

O tratamento térmico realizado entre os procedimentos, tem o objetivo de reestabelecer o equilíbrio termodinâmico no material e eliminar os sinais residuais para sua reutilização, de acordo com os dados definidos pelo fabricante. O forno utilizado foi o PTW modelo *Freiburg* (Figura 5), usando o protocolo de 10 minutos à temperatura de 240°C e, posteriormente, 10 segundos a 50°C, como recomendado pelo fabricante.

Figura 5: Forno PTW modelo Freiburg

Fonte: **Elaborado pela autora**

3.2.1.6 Posicionamento dos detectores TL no simulador

A cada aquisição tomográfica foram utilizados 4 detectores para medir radiação de fundo (*background*) e 91 detectores, posicionados da seguinte forma: um detector na região de interesse na parte interna do simulador antropomórfico (para avaliar a dose absorvida), e três na parte externa (para medir a dose na superfície de entrada), tanto do lado direito quanto do esquerdo, como apresentado na Figura 6 e Quadros 2 e 3 (SOBOTTA, 2000).

Figura 6: Posicionamento dos detectores TL no simulador

Fonte: **Elaborado pela autora**

Quadro 2: Posicionamento dos detectores TL no simulador para D

Dose Absorvida (D)				
Órgãos	**Fatia**	**Direita**	**Esquerda**	**Central**
Cérebro	3	1	1	
Cortical Óssea	3	1	1	
Cristalino	4	1	1	
Glândulas parótidas	5	1	1	
Glândulas Submandibulares e Sublinguais	6	1	1	
Mucosa Oral	6	1	1	
Linfonodo Cervical	8	1	1	
Tireoide	9	1	1	
Esôfago	13			1
Região Paraesternal	13	1	1	
Medula Óssea (centro do esterno)	14			1
Pulmão	14	1	1	
Mamas	16	1	1	
Fígado	18	1		
Estômago	19		1	
Cólon	21			1
	24	1	1	
Ovário	29	1	1	
Bexiga	30			1
Útero	30			1

Fonte: **Elaborado pela autora**

Quadro 3: Posicionamento dos detectores TL no simulador para ESD.

Dose de Superfície de Entrada (ESD)				
Órgãos	**Fatia**	**Direita**	**Esquerda**	**Central**
Cristalino	4	3	3	
Glândulas parótidas	5	3	3	
Glândulas Submandibulares e Sublinguais	6	3	3	
Mucosa Oral	6	3	3	
Linfonodo Cervical	8	3	3	
Tireoide	9			3
Região Paraesternal	13	3	3	
Mamas	16	3	3	
Fígado	18	3		
Estômago	19		3	
Cólon	24	3	3	
Bexiga	30			3

Fonte: **Elaborado pela autora**

3.2.2 Etapa da simulação do exame tomográfico

Os exames foram realizados no tomógrafo *Kodak* 9000C 3D com as seguintes especificações técnicas (Quadro 4):

Quadro 4: Especificações técnicas do Kodak 9000C 3D durante a simulação de exame da ATM no simulador

Especificações técnicas no exame	
Tensão do tubo	70 Kv
Corrente do tubo	10 Ma
Tempo de exposição (rotação)	10,8 segundos
Colimação (FOV)	5,0cm x 3,7cm
Tamanho do Voxel isotrópico	76x76x76µm
Ângulo do Alvo	5º
Filtração inerente	2,5mm eq. Al
Distância foco-detector	60cm

Fonte: **Elaborado pela autora**

O protocolo de aquisição de imagem para avaliação da ATM, em tomógrafos de feixe cônico de FOV menor apresentam 4 aquisições (Quadro 5):

Quadro 5: Protocolo de exame da ATM em tomógrafo de feixe cônico de FOV menor

Lado	Boca aberta	Boca fechada
Direito	1	1
Esquerdo	1	1

Fonte: **Elaborado pela autora**

Foram realizados 5 exames tomográficos totais para ATM, sendo que a cada exame total, os TLs irradiados foram recolhidos e levados à leitora *Harshaw* 5500 *Thermo Eléctron* para a obtenção dos valores das doses na superfície de entrada e adsorvida de cada região. Posteriormente, os TLs foram tratados termicamente no forno PTW modelo Freiburg para a realização do próximo exame.

O posicionamento do simulador *RANDO* feminino no tomógrafo *Kodak* 9000C 3D foi através do sensor de imagem do próprio equipamento, sendo inicialmente posicionada com o plano sagital mediano paralelo ao centro rotacional da unidade de feixe cónico para alinhar o simulador antropomórfico a região de interesse da ATM. Em todas as aquisições o simulador obteve o mesmo posicionamento vertical e horizontal (Figura 7).

Figura 7: Simulação do exame tomográfico

Fonte: **Elaborado pela autora**

3.3 Etapa dos cálculos

Foram realizadas as médias dos valores das doses na superfície de entrada (ESD) e doses absorvidas (D), dos 5 exames totais de ATM respectiva a cada região de interesse.

3.3.1. Dose na superfície de entrada (ESD)

É o kerma no ar no eixo do feixe de raios X no ponto onde este penetra no paciente ou no simulador. A contribuição da radiação retro-espalhada é incluída. A unidade de dose no Sistema Internacional (SI) é em *Gray* (Gy), correspondente a $J.Kg^{1}$(INTERNATIONAL COMMISSION THE RADIOLOGICAL PROTECTION, 1991).

3.3.2 Dose absorvida

É o quociente da energia média depositada pela radiação ionizante na matéria ($d\bar{\varepsilon}$) de massa (dm), num ponto de interesse, demonstrado pela equação 1. A unidade de dose no Sistema Internacional (SI) é o *Gray* (Gy), correspondente a $J.Kg^{-1}$ (INTERNATIONAL COMMISSION THE RADIOLOGICAL PROTECTION, 2007):

$$D = \frac{d\bar{\varepsilon}}{dm} \qquad (1)$$

Neste estudo, para a determinação da dose absorvida, utilizou-se a equação 2:

$$\mathrm{D_T} = D.\left(\frac{\mu en}{\rho}\right)_{tecido/ar} \qquad (2)$$

Na qual, D é o valor médio das leituras do detector TL em mGy, e $\mu en/\rho_{\,tecido/ar}$ é a relação entre os coeficientes de absorção de energia em massa de tecidos e ar para a energia média das qualidades dos exames.

Por meio da constituição elementar de cada órgão de interesse e do ar seco (ICRU 44,1989; WHITE et al 1987) apresentados na Tabela 1, foi utilizado o Programa online XCOM (National Institute of Standards and Technology - NIST) para obter o coeficiente de absorção de energia em massa de tecidos e do ar, tendo como referência a energia média do aparelho *Kodak* 9000C 3D (0,0368 MeV) obtida pelo programa XCOMP5R (NOWOTNY R.; HOFER A.,1985).

Tabela 1: Composição elementar de tecidos e órgãos do corpo (% por massa)

Locais	**H**	**C**	**N**	**O**	**Na**	**Mg**	**P**	**S**	**Cl**	**Ar**	**K**	**Ca**	**Fe**	**I**
Ar		<0.001	0.755	0.231						0.012				
Tecidos Moles*	0.106	0.315	0.024	0.547	0.001		0.002	0.003	0.002		0.002			
Tireoide	0.104	0.119	0.024	0.745	0.002		0.001	0.001	0.002		0.001			0.001
Trato Gastro**	0.100	0.222	0.022	0.644	0.001		0.002	0.003	0.001		0.004	0.001		
Gl. Salivares***	0.105	0.100	0.023	0.763	0.002		0.001	0.002	0.002		0.002			
Cortical óssea	0.034	0.1550	0.042	0.435	0.001	0.002	0.103	0.003	x			0.225		
Cérebro	0.107	0.145	0.022	0.712	0.002		0.004	0.002	0.003		0.003			
Mama	0.106	0.332	0.030	0.527	0.001		0.001	0.002	0.001					
Cristalino	0.096	0.195	0.057	0.646	0.001		0.001	0.003	0.001					
Pulmão	0.103	0.105	0.031	0.749	0.002		0.002	0.003	0.003		0.002			
Ovário	0.105	0.093	0.024	0.768	0.002		0.002	0.002	0.002		0.002			
Útero	0.102	0.143	0.034	0.710	0.001		0.002	0.003	0.001		0.004			
Medula Óssea	0.105	0.414	0.034	0.439			0.001	0.002	0.002		0.002		0.001	

*Tecidos moles feminino (pele, medula óssea, fígado, cérebro, intestino, pulmão, linfa, bexiga, tireoide, útero)
**Trato Gastrointestinal
*** Glândulas Salivares
Tabela adaptada do ICRU 44,1989 e WHITE et al.,1987.

Fonte: **Elaborado pela autora**

3.3.3 Dose equivalente

É o valor médio da dose absorvida ($D_{T,R}$) em um tecido ou órgão (T), obtido sobre todo o tecido ou órgão (T), devido à radiação (R), levando em consideração o fator de radiação (W_R) (Tabela 2), como demonstrado na equação 3:

$$H_T = \sum_R W_R \cdot D_{T,R} \qquad (3)$$

A unidade de dose no Sistema Internacional (SI) é em *Sievert* (Sv), equivalente a $J.Kg^{-1}$ (INTERNATIONAL COMMISSION THE RADIOLOGICAL PROTECTION, 2007).

Tabela 2: Fatores de ponderação da radiação recomendada pela ICRP 103

Tipo de radiação	Fator de ponderação da radiação, WR
Fótons	1
Elétrons e Muons	1
Prótons e pions carregados	2
Partículas α, fragmentos de fissão e núcleos pesados	20
Nêutrons	Uma função contínua de energia de nêutrons

Tabela adaptada da publicação ICRP 103, 2007

Fonte: **Elaborado pela autora**

3.3.4 Dose efetiva

É a soma ponderada das doses equivalentes em todos os tecidos ou órgãos do corpo, utilizando a equação 4:

$$E = \sum_T W_T \cdot H_T \qquad (4)$$

Na qual, W_T é o fator de peso para o tecido $_T$ (Tabela 3) e H_T é a dose equivalente a ele atribuída.

A unidade de dose no Sistema Internacional (SI) é em Sievert (Sv), equivalente a $J.Kg^{-1}$ (INTERNATIONAL COMMISSION THE RADIOLOGICAL PROTECTION, 2007).

Tabela 3: Fator de ponderação dos tecidos recomendados

Tecido	WT
Medula óssea, cólon, pulmão, estômago, mama, resto dos tecidos*	0,12
Gônodas	0,08
Bexiga, esôfago, fígado, tireoide	0,04
Superficie do osso, cérebro, glândulas salivares e pele	0.01

*Restantes dos tecidos: Adrenais, Região Extratorácica, Vesícula, Coração, Rins, Nódulos Linfáticos, Músculo, Mucosa Oral, Pâncreas, Próstata, Intestino Delgado, Baço, Timo, Útero/Cérvix
Tabela adaptada da publicação ICRP 103, 2007

Fonte: **Elaborado pela autora**

3.3.5 Estimativa do risco radioinduzido de câncer e alterações morfofuncionais

Durante um exame tomográfico de feixe cônico para avaliação da ATM, foi utilizado o relato do *Biologic Effects of Ionizing Radiation* (NATIONAL RESEARCH COUNCIL, 2006).

3.3.5.1 Estimativa de risco radioinduzido de câncer - BEIR VII (2006)

Segundo o *National Research Council* - BEIR VII (2006), o modelo de risco linear sem limiar (LNT- linear no-threshold) descreveu a mais razoável descrição da relação entre a exposição de baixas doses de radiação ionizante e a incidência de canceres sólidos que são induzidos por radiação ionizante. O modelo linear-quadrático foi adotado pela comissão para a estimativa de leucemia.

A estimativa do risco radioinduzido de câncer, de acordo com o *National Research Council* - BEIR VII (2006) considera o sexo e a idade do paciente a exposição na radiação, sendo que o maior risco é para a sexo feminino e em indivíduos mais jovens. O cálculo é realizado de acordo com a equação 5:

$$R = r_T \, . H_T \qquad (5)$$

Onde: R compreende o risco efetivo de incidência de câncer, r_T é o risco de câncer específico para o tecido ou órgão (Tabela 4) e H_T que é a dose equivalente no tecido T.

Tabela 4: Risco de incidência de câncer por idade feminina: Número de caso de 100.000 pessoas expostas a uma dose de 0,1 Gy

ÓRGÃO	IDADE DE EXPOSIÇÃO						
	20	**30**	**40**	**50**	**60**	**70**	**80**
Estomago	52	36	35	32	27	19	11
Cólon	114	82	79	73	62	45	23
Fígado	14	10	10	9	7	5	2
Pulmão	346	242	240	230	201	147	77
Mama	429	253	141	70	31	12	4
Útero	26	18	16	13	9	5	2
Ovário	50	34	31	25	18	11	5
Bexiga	109	79	78	74	64	47	24
Tireoide	113	41	14	4	1	0.3	0.0
Leucemia	71	63	62	62	57	51	37
Todos os sólidos	1575	1002	824	678	529	358	177
Outros	323	207	181	148	109	68	30
Todos os canceres	1646	1065	886	740	586	409	214

Tabela adaptada da publicação BEIR VII, 2006
Obs: Número de caso por 100.000 pessoas expostas por uma dose de 0,1 Gy.

Fonte: **Elaborado pela autora**

Estas estimativas são obtidas como estimativas combinadas baseadas no risco relativo e risco absoluto, ajustado pelo DDREF de 1,5, exceto para leucemia, que é baseada no modelo linear quadrático.

4 ARTIGOS

4.1 Artigo 1

Dose de radiação em pacientes submetidos em exames TCFC para avaliação de ATM: Revisão Sistemática.

Artigo será submetido à **Radiologia Brasileira** (Qualis B2)**,** cujas normas para submissão de artigos podem ser visualizadas no endereço eletrônico:

Doses de radiação em pacientes submetidos em exames TCFC para avaliação de ATM: Revisão Sistemática.

Radiation dose in patients submitted to CBCT exams for ATM evaluation: Contemporary literature

Carolina Drumond de Barros e Azevedo[1], Madelon Aparecida Fernandes Zenóbio[2], Maria do Socorro Nogueira[2], Flávio Ricardo Manzi[3], Élton Gonçalves Zenóbio[3].

C D B Azevedo[1]; M A F Zenóbio[2]; M S Nogueira[2]; FR Manzi[3]; E G Zenóbio[3]*

[1]Programa de Pós-graduação em Odontologia - Mestrado em Clínicas Odontológicas da Pontifícia Universidade Católica de Minas Gerais, Belo Horizonte, MG, Brasil; [2]Centro de Desenvolvimento da Tecnologia Nuclear- CDTN/CNEN, Belo Horizonte, MG, Brasil; [3]Departamento de Odontologia da Pontifícia Universidade Católica de Minas Gerais, Belo Horizonte, MG, Brasil.

*Correspondência para o autor:

•Dr. Elton Gonçalves Zenóbio. Av. Dom José Gaspar, Prédio 46 - Programa de Pós-graduação em Odontologia, Coração Eucarístico, Belo Horizonte – MG - CEP: 30535-901 - Telefone: 55 31 33194414 - zenobio@pucminas.br

RESUMO

O objetivo desta revisão de literatura foi avaliar e comparar, nos estudos identificados na literatura, os valores das doses de radiação em exame de tomografia computadorizada de feixe cônico (TCFC) específicos na avaliação da articulação temporomandibular (ATM). Materiais e métodos: O presente estudo se baseou na base de dados eletrônica PubMed para localizar e identificar relatos de pesquisa sobre dosimetria em TCFC nos protocolos de exame para a avaliação de imagens de ATM, retrospectivamente até o ano de 2011. Resultados: Por meio da pesquisa realizada em novembro de 2016, foram obtidos 40 artigos, porém somente 6 desses são restritos aos últimos 5 anos e foram inclusos na revisão de literatura, pois são estudos em que o tema e a metodologia são referentes a dosimetria em TCFC para avaliação de ATM. Conclusão: A seleção do exame tomográfico deve ser realizada de modo adequado, controlando os parâmetros de exposição de acordo com cada paciente. Os órgãos com maior exposição são: glândulas parótidas, cristalinos, glândulas submandibulares e cérebro. Pesquisas de dosimetria em pacientes devem buscar uma padronização na metodologia, para se comparar diretamente os valores obtidos entre estudos, e também a otimização das doses de radiação e modelos de proteção em pacientes.

Palavras-chave: Tomografia Computadorizada de Feixe Cônico, Dosimetria. Articulação Temporomandibular. Dose efetiva, Dose absorvida, Dose de radiação.

ABSTRACT

The objective of this literature review was to evaluate and compare the radiation dose values in a cone beam computed tomography (CBCT) test to evaluate temporomandibular joint (TMJ) in the literature in the last five years. Materials and methods: The present study was based on the PubMed electronic database to locate and identify reports on BMC dosimetry research in the examination protocols for the evaluation of TMJ images, retrospectively up to the year 2011. Results: Through the research Carried out in November 2016, forty articles were obtained, but only 6 of these were restricted to the last five years and were included in the literature review, since they are studies in which the subject and the methodology are referring to dosimetry in CBCT for TMJ evaluation. Conclusion: The selection of the CT scan should be performed in an appropriate manner, controlling the exposure parameters according to each patient. Patient dosimetry studies should continue to seek standardization in the methodology (so that it can directly compare the values obtained between studies) and also the optimization of the radiation dose in patients.

Keywords: Cone-Beam Computed Tomography, Dosimetry, Temporomandibular Joint, Radiation dose, Effective dose, Absorved dose.

Introduction

The Cone-Beam Computed Tomography (CBCT), for dentomaxillofacial region, is used as a diagnosis and treatment planning tool in the area of dental clinics, otorhinolaryngological and polyclinic orthopedic clinics that in the past were not typically associated with CT[(1)]. This mode of examination offers three-dimensional images of the hard tissue with higher spatial resolution, almost totally free of overlapping, offering significant advantages in relation to the image quality and quantity of the anatomical regions visualized, as well as, lower doses of radiation to the patient and lower cost to the population when compared to the Multislice CT (MSCT)[(2, 3)].

The use of the CBCT examination is based on a concise cases, the knowledge of radiation doses and the requirements of radiation protection, since the radio induced risk of cancer and morphofunctional changes to organs and tissues exposed to radiation should be considered for this new modality of exam[(1, 4, 5,6)].

The objective of this literature review was to evaluate and compare the values of radiation doses in concomitant beam computed tomography (CBCT) for evaluation of temporomandibular joint (TMJ) reported in the literature in the last five years.

The state of the art in the literature addresses the aspects related to the importance of knowledge in the dental practice of this modality of diagnostic imaging and the issues related to the dosimetry of the radiations and the determination of the levels of diagnostic references. Authors were dedicated to consolidate, through systematic reviews, the state of the art in CBCT, addressing theoretical and methodological aspects. Can be cited:

- Vos et al (2009)[7], analyzed the literature on the CBCT of the oral and maxillofacial region, from 1998 to 2007, through the PUBMED research database. The study revealed 375 articles, 176 of which were clinically relevant and analyzed in detail. The results of this systematic review show that there is an inconsistency in reported terminology for CFCT properties and configurations. There is still a lack of evidence-based data on radiation doses for CBCT. Based on the results of this study, a minimum set of parameters is proposed as a guideline for future studies.
- Li (2013)[8], analyzed 30 articles to deepen and understand the risk of CBCT, the effective doses in intraoral radiography, panoramic radiography, lateral and postero-anterior cephaladiography, CBCT. The protective effect of the thyroid protector and pumblic glasses has also been reviewed. According to this study, one conclusion that could be drawn is that the thyroid protector and umbilical goggles should be used during a CBCT examination, since diagnostic information and image quality are not reduced.
- Al-Okshi et al (2015)[9], analyzed the literature up to April 2014 on effective dose in cranial CTCT, emphasizing measurement methods and examination protocols, through the MEDLINE, The Cochrane Library and Web of Science databases. Thirty-eight studies were included, revealing the need for studies on dosimetry related to image quality.
- Ludlow et al (2015)[10], analyzed the English literature on effective dose and analysis of radiation dose measurements through the PubMed and EMBASE databases, yielding 519 and 743 publications respectively, of which only 20 of these were analyzed. They concluded that dosimetry research involves many variables. Decisions affecting these variables can have a profound impact on the accuracy, validity, and extensibility of results.

- Kiljunen et al (2015)[11], compared equipment based on the manufacturer's data, including scanner-specific X-ray spectra, image reconstruction and image quality issues in the CBCT, as well as addressing radiation dose and optimization issues. They also discussed clinical needs and what kind of professionals can operate CFCT systems safely, and issues that still need to be resolved as image quality. Collaboration between medical physicists, radiologists, clinicians and engineers is essential for optimization of radiation in modern radiology, also covering the use of CBCTs.
- Goulston et al (2016)[12], analyzed the literature from 1998 to May 25, 2015 on radiation dose reduction through kV and mAs in CBCT without affecting image quality. PubMed / MEDLINE and Ovid / EMBASE databases were used, with only 24 publications included for the systematic review. The authors concluded that many CBCT equipment should optimize one or more of the exposure parameters investigated, and thus reduce the radiation dose of the patient while maintaining diagnostic image quality. However, stricter dosimetry research is still needed.

Dosimetry studies and radioinducicide risks (State of the art)

The obtaining of a standard of measurement of the doses of the ionizing radiation has demonstrated the preoccupation with the radioprotection of the patient at the present time, especially with respect to the new modalities of diagnostic exams like the CBCT evaluated in this study of review of the literature[1,6,13,14].

The state of the art was based on researchs in which the authors performed as dose measurements the evaluation of absorbed and effective doses performed for the comparison of CBCT exams with other CT imaging and panoramic radiography.

As materials and methods, the authors used RANDO anthropomorphic simulators and thermoluminescent dosimeters positioned in the anatomical regions corresponding to human organs and tissues radiosensitive for measurement of radiation doses during the examination of CBCT[15-25] .

Zenóbio et al 2010[26] Evaluated the dose of entry into the skin in patients who would perform radiographic examinations for placement of implants. Two groups were separated, the first with seven patients submitted to panoramic radiography and conventional spiral CT in the Cranex Tome equipment (Soredex Helsinki, Finland), and the second with twelve patients submitted to CT helical CT scanning (Elscint, Haifa, Israel). The regions evaluated were the organs of the thyroid, parotid gland, submandibular and crystalline gland.

In some studies[15,16,17,19,20,21,22,23] The absorbed and / or effective doses were measured according to ICRP 60 and /or ICRP 103 and compared in CBCT examinations with panoramic examinations and /or computed tomography examinations to evaluate maxillary and mandibular images in protocols for dental implants using Anthropomorphic simulators.

Tsiklakis et al 2005[17] Applied in their study the comparison of the examination protocols using or not personal protective screening devices (EUREKA! - TRIX, Newtom) for the thyroid gland and the cervical spine. The estimated effective dose included the salivary glands.

The tomographs evaluated in the surveys were: NewTom 9000 (Aperio Inc, Sarasota, Fla), NewTom QR-DVT 9000 (Verona, Italy), NewTom 3G (Quantitative Radiology, Verona, Italy); CB Mercuray (Hitachi Medical of America, Twinsburg, OH); Promax 3D (Planmeca OY, Helsinki, Finnland); Prexion 3D (Terarecon, San Mateo, CA); Galileos (Sirona, Charlotte, NC); Classic i-CAT (Imaging Sciences International, Hatfield, PA); Next Generation i-CAT (Imaging Sciences International); Iluma (Imtec Imaging, Ardmore, OK), Accuitomo 3D (J. Morita Corporation, Kyoto, Japan), i-CAT (Imaging Sciences International, Hatfield, Pennsylvania, USA); 3D Accuitomo 170, Galileos Confort, Iluma Elite, Kodak 9000 3D, Kodak 9500, NewTom VG, NewTom VGi, Pax-Uni3D, Picasso Trio, Scanora 3D, SkyView, Veraviewepocs 3D, ProMax 3D Gendex GXCB 500 Sirona Orthophos XG Carestream health CS 9000, Care stream 9300 scanner (Care stream Health)[(15,16,17,18,19,20, 21,22,23,24,25)] .

The absorbed and effective dose values were compared with the exams performed on multislice tomograph *Somatom Sensation* 32-row/64-*slice configuration* (*Siemens Medical Solutions* USA, Malvern, PA)[(18)], Spiral conventional tomograph Scanora (*Orion Corporation Soredex*, Helsinki, Finlândia), CT *Multislice Spiral HiSpeed/Fxi* (*General Electric*, *Milwaukee*) (Chau et al 2009), MSCT in the tomographs Somatom Volume Zoom 4(*Siemens*, *Erlangen*, Alemanha), Somatom Sensation 16 (*Siemens*, *Erlangen*, Alemanha) e M×8000 IDT (Philips Medical Systems, Best, the Netherlands)[(20)] e TC Multislice SAFIRE (Siemens, Erlangen, Alemanha)[(25)] . The effective dose between studies[15-18,20-23] is in the table 1.

Table 1: Effective dose comparison between studies[15-18,20-23]

Author/Year	Equipment	Calculation	Effective Dose
Ludlow et al 2003[(15)]	**Panoramic:** Orthophos Plus DS **CBCT**: NewTom QR-DVT 9000	ICRP 60	**Panoramic:** 6,2µSv **CBCT:** **Jaw:** 19,9µSv **Mandíble:** 34,7µSv **Maxilla and Mandíble#1:** 36,9µSv **Maxila and Mandíble#2:** 42,1µSv
Mah et al 2003[(16)]	NewTom 9000	ICRP 60	**Maxilla and Mandíble:** 50,3µSv
Tsiklakis et al 2005[(17)]		ICRP 60	**Não-blindagem**:0,035mSv **Com blindagem (Pb):**0,023mSv
Ludlow et al 2008[(18)]	**FOV large:** NewTom 3G; CB Mercuray; Next Generation i-CAT; Ilumina **FOV medium:** Galileos; Classic i-CAT; **FOV smal:**	ICRP 60 ICRP 103	**CBCT:** **FOV large:** NewTom 3G: 42µSv (ICRP 60); 68µSv (ICRP 103) CB Mercuray(high quality): 806µSv (ICRP 60); 1073µSv (ICRP 103) CB Mercuray (low quality): 464µSv (ICRP 60), 569µSv (ICRP 103 Next Generation i-CAT: 37µSv (ICRP 60); 74µSv

	Promax 3D; Prexion 3D; **MSCT:** Somatom Sensation 32-row/64-slice Configuration		Ilumina standard: 50µSv(ICRP 60); 98µSv(ICRP 103) Ilumina ultra: 252µSv(ICRP 60); 498µSv(ICRP 103) **FOV medium:** Classic i-CAT; 29µSv(ICRP 60); 69µSv(ICRP 103) **FOV smal:** Promax 3D small adult: 151µSv(ICRP 60); 488µSv(ICRP 103) Promax 3D large adult; 203µSv(ICRP 60); 652µSv; (ICRP 103) Prexion 3D low exposure: 66µSv(ICRP 60); 189µSv(ICRP 103) Prexion 3D high resolution: 154µSv(ICRP 60); 388µSv(ICRP 103) **MSCT:** Somatom Sensation 64-slice: 453µSv(ICRP 60); 860µSv(ICRP 103) Somatom Sensation 64-slice com CARE dose 4D: 85µSv(ICRP 60); 534µSv(ICRP 103)
Loubele et al 2009[20]	**CBCT:** Accuitomo3D; NewTom 3G; i-CAT; **MSCT:** Somatom Volumezoom4; Somatom Sensation 16; Mx8000 IDT;	ICRP 103	**CBCT:** Accuitomo3D: Maxilla: Previous Tooth: 29µSv Premolar and canine: 44µSv Molar:29µSv Mandible: Previous tooth (maxilla): 13µSv Premolar and canine:22µSv Molar:29µSv NewTom 3G; 6” FOV 57µSv 12” FOV 30µSv i-CAT; 13cm 10s 48µSv 13cm 40s 77µSv FOV extended 82µSv **MSCT:** Somatom Volumezoom4; 494-1110µSv Somatom Sensation 16; 474-995µSv Mx8000 IDT; 541-1160µSv
Qu et al 2010[21]	ProMax 3D	ICRP 103	102-298µSv
Davies et al 2012[22]		ICRP 103	FOV large:78µSv FOV 13cm: 77µSv FOV 6cm: 58-113µSv
Pauwels et al 2012[23]		ICRP 103	19-368µSv

Qu et al 2010[21] performed different dental protocols defined by the different combinations of patient size, volume size and image resolution. There were five standard patient sizes setting the milliampere (mA) from 8mA to 16mA. The largest volume was 80x80mm (diameter per height), aiming to include the upper and lower jaw region, the intermediate volume of 50x80mm, used for examination of the maxilla or mandible and the smallest volume of 50x40mm, applied in the examination of sextants Of individual arcs. The selectable resolutions available were low, normal, and high.

Ludlow et al 2003[(15)] Notes that the tomographic examination resulted in an effective dose 3-7 times greater than that notes in the panoramic examination.

Mah et al 2003[(16)] Obtained, according to them, a lower value than that obtained with other computed tomography imaging methods. In their study they concluded that it should be borne in mind that the data are not directly comparable, due to many differences between studies, and recommend the standardization of parameters and methods whenever possible (anatomical areas analyzed, the composition of the anthropomorphic simulator, the Location of dosimeters) to ensure more direct and significant comparisons.

Tsiklakis et al 2005[(17)] Through their study, notes a reduction of the doses absorbed in the regions of the thyroid and cervical spine, and also in the effective dose with the use of lead protection.

Ludlow et al 2008[(18)], Concluded that CBCT may be recommended as a lower dose technique when compared to medical CT scans for maxillofacial exams. Comparing the effective doses calculated by ICRP 103 (2007) for standard dentomaxilofacail evaluation, the MSCT obtained doses of 1.5 to 12.3 times higher than the medium FOV CBCT.

Chau et al 2009[(19)] notes that spiral multislice CT obtained the highest absorbed dose to organs when compared to CBCT. Regardless of the study protocol in the study, the salivary glands had the highest absorbed dose values.

Loubele et al 2009[20] Notes that the effective dose levels in the CBCT examination remained lower than the MSCT clinical protocols, being extremely important the justification and selection of the examination to optimize the dose of radiation in the patient, as well as to obtain an adequate image quality for the diagnosis.

Qu et al 2010[21] when scanning with the low resolution settings, effective doses were significantly reduced ($p = 0.05$). Effective dose reduction can be achieved when using low exposure parameters. The ProMax 3D scanner showed good reproducibility. Filtration added in the beam significantly reduced the effective dose on the Promax 3D examination. Choice of patient size, FOV and resolution can affect patient exposure by an order of magnitude. Therefore, the selection of each of these parameters must be careful and necessary to optimize the effective dose of the patient.

Zenóbio et al 2010[26] Obtained in panoramic examination, the maximum absorbed doses near the regions of the parotid glands, being 1,57mGy on the right and 1,89mGy on the left. In the conventional spiral CT scan, the maximum absorbed dose was 4,41mGy near the right and left parotid glands, while near the right or left submandibular gland, the maximum absorbed doses reached 40,7mGy. In helical computed tomography for mandibular and maxillary exams, the maximum absorbed dose was 40,9mGy near the parotid glands and 41,0mGy near the submandibular gland. Close to the lens and thyroid, absorbed doses were less than 0,23mGy in all exams. In the study, regardless of the target area of the examination, the submandibular and parotid glands were the most irradiated organs. The authors suggested that efforts should be made by professionals to optimize radiation doses to the patient without losing the information necessary for treatment planning. All the techniques evaluated presented values of radiation doses considerably higher in the salivary glands (parotid and submandibular) when compared to the thyroid and crystalline glands. Helicoid computed tomography, compared to panoramic radiography and conventional spiral tomography, was the technique with the highest radiation dose for patients.

Davies et al 2012[22] When comparing several datasets of different researchers, the authors support the need for very careful control in methods for measurement, even if they feel that variation in values between studies is unavoidable. Therefore, it would be prudent for them to use the same standardized experimental protocol.

Pauwels et al 2012[23], conducted a dosimetry study evaluating examination protocols for total maxilla, anterior teeth region, total mandible and molar region in CBCT. There was a wide range of apparent measurement values across all organs due to differences in exposure factors, diameter and height of the primary beam, and positioning of the beam relative to radiosensitive organs. The results showed a distinction between the small, medium and large FOV CBCT scanners, in addition to the different protocols, as applied to the different indication groups. According to the authors, the effective dose received is strongly related to the size of the FOV. The results of the present study indicate that effective dose optimization should be performed by appropriate selection of exposure parameters and FOV size, depending on diagnostic needs.

Materials and methods

The present study was based on the PubMed electronic database to locate and identify reports on CBCT dosimetry in the examination protocols for the evaluation of TMJ images, retrospectively up to the year 2011, using the following keywords: "Cone -Beam Computed Tomography, "" Dosimetry, "" Temporomandibular Joint, "" Radiation dose, "" effective dose, "" absorbed dose. " The search was limited to articles written in English.

Articles identified by the initial search strategy were independently assessed by two authors in the area who agreed on the following inclusion criteria: 1-population (cranium, patients or anthropomorphic simulators), 2-intervention (concomitant computed tomography, thermoluminescent dosimeters, Of ionization), 3-endpoint (measurement of radiation dose and radio-induced risk of cancer during CBCT examination).

Results

The research was carried out in November 2016, when 40 articles were obtained, but only six of these studies, referring to the subject and the methodology, dosimetry in CBCT for total evaluation of TMJ, restricted to the last five years were included in the present literature review. Of these six articles, one was published in 2015(27), another in 2014(28), two in 2013 (29,30),one in 2012(31) and another in 2011(32). Four of these were published by Dentomaxillofacial Radiology(27,28,29,30), and the others in the American Journal of Orthodontics and Dentofacial Orthopedics(32), Japanese Journal of Radiological Technology(31) (Nihon Hoshasen Gijutsu Gakkai Zasshi*)*, as can be seen in Table 1.

Table 1. Selected articles:

	Autor (es)	**Título**	**Periódico**	**Ano**
1	Kadesjö N, Benchimol D, Falahat B, Näsström K, Shi XQ [27]	Evaluation of the effective dose of cone beam CT and multislice CT for temporomandibular joint examinations at optimized exposure levels	Dentomaxillofacial Radiology	2015
2	Shin, KC; Nam,H; Park, HU; Choi, HY; Kim and CS Park [28]	Effective doses from panoramic radiography and CBCT (cone beam CT) using dose area product (DAP) in dentistry	Dentomaxillofacial Radiology	2014
3	Lukat TD, Wong JC, Lam EW [29]	Small field of view cone beam CT temporomandibular joint imaging dosimetry	Dentomaxillofacial Radiology	2013
4	A Al-Okshi, M Nilsson, A Petersson, M Wiese and C Lindh [30]	Using GafChromic film to estimate the effective dose from dental cone beam CT and panoramic radiography	Dentomaxillofacial Radiology	2013
5	Okano T, Matsuo A, Gotoh K, Yokoi M, Hirukawa A, Okumura S, Koyama S [31]	Comparison of Absorbed and Effective Dose from Two Dental Cone Beam Computed Tomography Scanners	Japanese Journal of Radiological Technology (Nihon Hoshasen Gijutsu Gakkai Zasshi)	2012
6	Librizzi ZT 1 , Tadinada AS, Valiyaparambil JV, Lurie AG, Mallya SM [32]	Cone-beam computed tomography to detect erosions of the temporomandibular joint: Effect of field of view and voxel size on diagnostic efficacy and effective dose	American Journal of Orthodontics and Dentofacial Orthopedics	2011

Source: PubMed, 2016

Discussion

To better understand the articles identified by the research in PubMed were analyzed with details of the descriptors used by the authors, model / patient, methods used and analysis, presented by the table 2.

Table 2. Detailed analysis of selected articles

Continua

	Keywords (key words)	Model/ patient	Methods (materials)	Analysis	Conclusion
1	Keywords: temporomandibular joint; cone beam computed tomography; thermoluminescent Dosimetry	Alderson RANDO® Adult Male Anthropomorphic Simulator (Alderson Research Laboratories, New York, NY) Regions corresponding to organs for analysis: active bone marrow, brain, endothelium, esophagus, extrathoracic airways, lymph nodes, oral mucosa, salivary glands and thyroid.	They used the CBCT Promax 3D scanner (Planmeca, Helsinki, Finland); And the MSCT GE LightSpeed VCT (GE Healthcare, Little Chalfont, UK) 64 channels; To obtain dose values in the corresponding regions, they used TLD-100 thermoluminescent dosemeters (TLDs), read with the Harshaw 5500 reader (Thermo Scientific, Waltham, MA). The calculation of the effective dose was performed according to the publication of ICRP103	The interclass correlation was 0,999 and 0,998 for CBCT and MSCT, respectively. The LightSpeed VCT test resulted in higher effective doses for all organs except the salivary glands and lymph nodes, with an effective dose 20% higher than a Promax 3D examination. The effective dose estimated using the optimized exposure parameters was 92µSv for a bilateral TMJ examination in Promax 3D and 124µSv for the VCT LightSpeed	The effective doses determined for Promax 3D CBCT and LightSpeed VCT MSCT were 92 and 124 µSv, respectively. The use of FOV and adequate exposure parameters are essential for optimization and low effective dose.
2	Keywords: CBCT (cone beam CT); effective dose; ICRP; DAP (dose area product); conversion factor	DAP meter (VacuDAP; VacuTec Meßtechnik GmbH, Dresden, Germany) at the center of the X-ray beam.	They used the panoramic equipment CRANEX® 31 CEPH (Soredex Orion Corporation, Helsinki, Finland - panoramic) and the Alphard 3030 (Asahi Roentgen Ind. Co., Kyoto, Japan) and Rayscan Symphony (RAY Co., Suwon , Republic of Korea) with 4 different FOVs, depending on the purpose of the examination.	Comparison between dose values. Reproducibility of the examination: RaySafe Xi (Unfors RaySafe AB, Billdal, Sweden). The DAP value in adult panoramic radiography on CRANEX 31 CEPH was 79,9mGycm² and the effective dose was 6,39µSv. In the Alphard 3030 DAP value the "Cefalo" mode showed the highest DAP value with 3349mGy cm² and 428,3µSv in adults and 2001mGycm² and 255,9µSv in children. In the Rayscan Symphony tomograph the DAP value was 1126mGycm² And effective dose of 160,3µSv in adults and 1006mGycm² and 143,2µSv in children.	The effective doses of CBCT were superior to those of panoramic radiography. The differences in effective doses between the adult and child in the CBCT depended on the type of equipment and the exposure parameters used. Therefore, it is necessary that the selection of the examination is adequate, controlling the exposure. Research to minimize the effective dose in patients, especially children, should continue.

(Continuação)

	Keywords (key words)	Model/ patient	Methods (materials)	Analysis	Conclusion
3	Keywords: temporomandibular joint; cone beam computed tomography; radiation dosimetry	Anthropomorphic simulator RANDO (Alderson Research Laboratories, Stanford, CT), male model. Regions corresponding to organs for analysis: anterior, posterior and left cranial cap, center of cervical spine, body and branch of right and left mandible, right and middle surfaces of the thyroid, esophagus, right and left crystals, right cheek, nape of the side Left, right and left parotid, sublingual and submandibular glands, pituitary fossa, right and left orbit, pharynx and midbrain.	Hitachi CB MercuRay Cone Beam Tomographers (Hitachi Medical Systems, Tokyo, Japan); Kodak 9000® 3D (Carestream, Rochester, NY). The effective dose was estimated using ICRP 103 (2007).	The effective dose in the CB MercuRay tomograph was 223,6µSv, with Kodak 9000 3D of 20,5µSv. The difference between the effective doses were performed by ANOVA one-way analysis of variance ($p<0,0001$). Tukey's post-hoc analysis showed that all bilateral acquisition groups differed significantly from each other ($p<0,05$).	Acquisitions of individual right and left TMJ volumes using the Kodak 9000 CBCT 3D imaging system resulted in a more than tenfold effective dose reduction compared to the larger single field acquisition with the Hitachi CB MercuRay. This decrease becomes even more significant when using the lower pipe potential and the pipe current configurations.
4	Keywords: radiation dosage; cone beam computed tomography; film dosimetry	Anthropomorphic Simulator (RANDO® Phantom, The Phantom Laboratory, Salem, NY). Regions corresponding to organs for analysis: parotid glands, oral mucosa, extrathoracic airways, brain, cortical bone, red bone marrow, skin and thyroid.	The CBCT units used were Veraviewepocs 3De® (J Morita MFG Corp., Kyoto, Japan), ProMax® 3D (Planmeca, Helsinki, Finland) and NewTom VGi® (Quantitative Radiology, Verona, Italy). GafChromic XR-QA2 films were placed between the source and the simulator. The effective dose was estimated using ICRP 103 (2007).	The highest absorbed dose values were for the parotid glands in all analysis equipment. The lowest effective dose value was the ProMax 3D FOV smal conical beam tomograph at the total maxillary exam with 10µSv. The highest value was from the NewTom VGi medium FOV conic beam scanner in the high resolution TMJ scan with 129µSv.	In conclusion, the film GafChromic can be used to map the distribution and measure the absorbed dose of organ / tissue in CBCT and panoramic radiography. The use of small FOV and standard resolution reduces the effective dose when compared to FOVs or higher resolution.

(Conclusão)

	Keywords (key words)	Model/ patient	Methods (materials)	Analysis	Conclusion
5	Key words: cone beam computed tomography (CBCT), absorbed doses, effective doses, field of view (FOV)	Anthropomorphic simulator Alderson RANDO; The corresponding organs were: bone marrow, colon, adrenal, extrathoracic region, lung, gallbladder, stomach, heart, sinus, kidney, gonads, muscle, bladder, oral mucosa, esophagus, pancreas, liver, Prostate, thyroid, small intestine, bone surface, spleen, brain, thymus, salivary gland, uterus, skin.	The Alphard VEGA and 3DX MULTI-IMAGEMICRO CT were used. The calculation of the effective dose was performed according to the publications of ICRP 60 (1990) and 103 (2007).	The effective doses for the Alphard VEGA in D, I, P and C mode were 86, 238, 413, and 323μSv, respectively. Effective doses using 3DX for upper incisor, upper molar, mandibular incisor, mandibular molar and TMJ were 27, 30, 48, 60 and 14μSv, respectively.	Both the value of Alphard VEGA and that of 3DX revealed that the doses absorbed for the salivary glands and oral mucosa are much higher than the other tissues. You must select a suitable mode to perform the optimization..
6	Not included	16 dry, toothed or partially dentate human skulls, 16 TMJs with natural or artificially created erosions and 16 normal TMJs. Anthropomorphic head and neck simulator (RANDO, The Phantom Laboratory, Salem, NY). Regions corresponding to organs for analysis anterior, posterior, right and left cranial cap, center of cervical spine, body and branch of right and left mandible, surface and midline of thyroid, esophagus, right and left crystalline, right cheek, nape of the side Left, right and left parotid and submandibular glands, sublingual gland, pituitary fossa, right and left orbits and midbrain.	Maxilla and jaw positioned and fixed in occlusion with an elastic. Two acrylic plates (0,5") were placed between the X-ray source and the skull to simulate the absorption of soft tissues. The CBCT used was the Hitachi CB MercuRay CBCT scanner. 3 different imaging protocols were performed, with FOV and the size of the reconstructed voxels. TLD 100 dosimeters (Landauer, Glenwood, Ill) were positioned in the simulator. For a more accurate absorbed dose, 3 exams of each protocol were performed. The effective doses for each test were calculated according to ICRP 103 (2007)	The ROC curve was used to compare the values between equipment of different FOV sizes. The area under the curve for FOV 6in was statistically larger than that of FOV 12in ($p \leq 0{,}05$).	The diagnostic efficacy of CBCT scans for evaluation of erosive changes in TMJ is greater for the 6-in FOV and lower for the 12-in FOV.

The key words used by the authors were: temporomandibular joint, conical beam computed tomography, thermoluminescent dosimetry, CBCT, effective dose, ICRP, DAP (area product dose), conversion factor, radiation dosimetry, Dose of radiation, dosimetric film; Absorbed dose, effective dose, field of view (FOV). Of these, the most used by the authors was computed tomography of the conic bundle (four times) and temporomandibular joint (twice). The others were used only once each.

Four of the six studies used the Alderson RANDO anthropomorphic simulator to position the thermoluminescent dosimeters during the measurements of absorbed doses in organs and tissues(27,29,31,32). In a study(30), The RANDO anthropomorphic simulator was used, but the average of the absorbed doses was obtained using the GafCromic dosimetric film between the source and the anthropomorphic simulator. In another study(28) The method used to obtain the absorbed doses was with the DAP VacuDAP meter (VacuTec Meßtechnik GmbH, Dresden, Germany) in the center of the X-ray beam.

The region most evaluated was the one corresponding to the organ of the thyroid and salivary glands(27,29,30,31,32) followed by the esophagus(27,29,31,32). The least evaluated among the studies were the pharynx, lung, colon, adrenal glands, gall bladder, stomach, heart, breasts, kidneys, gonads, muscle, bladder, pancreas, prostate, small intestine, spleen and thymus(31).

Regarding the tomographs used, Kadejö et al(27) carried out their research on Promax® 3D tomographs (Planmeca, Helsinki, Finland -TCCB); GE LightSpeed VCT (GE Healthcare, Little Chalfont, UK- 64-slice TC). Shin et al.(28) used the CRANEX® 31 CEPH (Soredex Orion Corporation, Helsínquia, Finlândia – panorâmica) and Alphard 3030 (Asahi Roentgen Ind., Co. Ltd, Kyoto, Japão -TCCB) and Rayscan Symphony (RAY Co., Suwon, República da Coreia -TCCB) with 4 different FOVs, for facial, broad, mandibular or TMJ examinations and whether it was for adults or children. Lukat et al.(29) used Hitachi

CB MercuRay (Hitachi Medical Systems, Tóquio, Japão) and Kodak 9000® 3D (Carestream, Rochester, NY). Al-Okshi et al.[30] used the CBCT units Veraviewepocs 3De® (J Morita MFG Corp., Quioto, Japão), ProMax® 3D (Planmeca, Helsinki, Finlândia) and NewTom VGi® (Quantitative Radiology, Verona, Itália). Okano et al[31] used Alphard VEGA (modelo Alphard-3030; Asahi Les Ntogen Kogyo Co., Ltd.) and 3DX MULTI-IMAGEMICRO TC ((formula type MCT-1; Co., Ltd. Morita Seisakusho). Librizzi et al[32] used the Hitachi CB MercuRay CBCT scanner.

The ProMax 3D scanner (Planmeca, Helsinki, Finlândia)[27,30] and the Hitachi CB MercuRay CBCT scanner[29,32] were the most used among the 6 studies.

For the calculation of effective doses, the recommendations of the ICRP 103 were used in five[27,29,30,31,32] of the six studies, and the study by Shin et al.[28] was the only one that used the DAP measurement.

Kadejö et al.[27] notes that the effective doses determined for Promax 3D CBCT and LightSpeed VCT MSCT were 92µSv and 124µSv, respectively, and it was notes that the use of FOV and adequate exposure parameters are essential to obtain a low effective dose. In the study by Shin et al.[28] , the values of the effective doses in the CBCT exams were superior to those of panoramic radiography. There were also differences in the effective doses between the adult and child in the CBCT related to the equipment and the exposure parameters. The authors noted that selection of appropriate exposure parameters and control of radiation exposure are necessary to minimize effective dose to patients, especially children who are more radiosensitive. In this context, Lukat et al.[29] notes that the effective dose was ten times lower in the acquisitions of individual right and left TMJ volumes using the Kodak 9000 3D CBCT compared to the larger FOV acquisition using the Hitachi CB MercuRay tomograph. This behavior becomes even more significant when we use low exposure parameters. For Okano et al.[31] The doses absorbed in the salivary glands and oral mucosa are much higher than in the other tissues in examinations performed in Alphar and 3DX tomographers. The authors notes the need to select adequately the settings of the exposure parameters to perform the examination and to obtain optimization of radiation doses in the patients.

Regarding detection, Al-Okshi et al.[30] concluded that the GafChromic film can be used to map the distribution and measurement of the absorbed dose of organ / tissue in CBCT and panoramic radiography examinations. Using small FOV at standard resolution reduces the dose when compared to larger FOVs of the same ROI or higher resolution.

Librizzi et al.[32] estimated the effective doses administered by the various CFCT exams for a typical TMJ and craniofacial evaluation exam. The authors also notes better diagnostic efficacy of CBCT scans for the evaluation of erosive changes in TMJ 6-in FOV than 12-in FOV.

Final considerations

Considering the present literature review, it can be inferred that the use of FOV and adequate exposure parameters are essential to obtain radiation dose optimization in patients. The salivary glands obtained higher dose values compared to the other organs during a CBCT examination for the dentomaxillofacial region. Therefore, the selection of the examination should be performed adequately, controlling the exposure parameters according to each patient. Dosimetry studies in patients should continue to seek a standardization of the methodology, for the direct comparison of the values obtained between the studies, and also the optimization of the radiation dose in the patients.

REFERENCES

1. European Commission. Radiation protection safety and efficacy of a new and emerging dental X-ray modality (SEDENTEXCT). Project Final Report, 2012. Disponível em: <http://www.sedentexct.eu/files/radiation_protection_172.pdf>. Acesso em: 25 Aug. 2015
2. Scarf WC, Farman AG, Sukovic, P. Clinical applications of cone-beam computed tomography in dental practice. J Can Dent Assoc. 2006; 72: 75-80.
3. Zhang ZL, Cheng JG, Li G, Shi XQ, Zhang JZ, Zhang ZY, Ma XC. Detection accuracy of condylar bony defects in Promax 3D cone beam CT images scanned with different protocols. Dentomaxillofac Radiol. 2013; 42: 1-6.
4. National Research Council. Health risks from exposure to low levels of ionizing radiation: BEIR VII phase 2. *Washington, USA: The Nacional Academy of Sciences, 2006.*
5. International Commission the Radiological Protection. Recommendations of the international commission on radiological protection. In: Annals of ICRP. Oxford: Pergamon Press, 1991, vol.22, n.1/3, ICRP 60.
6. International Commission the Radiological Protection. Recommendations of the international commission on radiological protection. In: Annals of the ICRP. Oxford: Pergamon Press, 2007, vol.37, n.2-4, ICRP 103.
7. Vos WD, Casselman J, Swennen GRJ. Cone-beam computerized tomography (CBCT) imaging of the oral and maxillofacial region: A systematic review of the literature. Int J Oral Maxillofac Surg. 2009; 38: 609-25.
8. Li G. Patient radiation dose and protection from cone-beam computed tomography. Imag Sci Dent. 2013; 43: 63-9.
9. Al-Okshi A, Lindh C, Sal´e H, Gunnarsson M, Rohlin M. Effective dose of cone beam CT (CBCT) of the facial skeleton: a systematic review. Br J Radiol. 2015; 88: 20140658.

10. Ludlow JB, Timothy R, Walker C, Hunter R, Benavides E, Samuelson DB, et al. Effective dose of dental CBCT—a meta analysis of published data and additional data for nine CBCT units. Dentomaxillofac Radiol. 2015; 44: 20140197.
11. Kiljunen, Kaasalainen T, Suomalainen A, Kortesniemi M. Dental cone beam CT: A review. Phys Med. 2015; 31:844-60.
12. Goulston R, Davies J, Horner K, Murphy F. Dose optimization by altering the operating potential and tube current exposure time product in dental cone beam CT: a systematic review. 2016;45: 20150254.
13. International Atomic Energy Agency. Human Health Reports Nº5: Status of computed tomography dosimetry for wide cone beam scanners. Viena: IAEA, 2011. Disponível em: http://www.iaea.org/Publications/index.html.
14. Health Protection Agency. Working Party on Dental Cone Beam CT Equipament: Guidance on the Safe Use of Dental Cone Beam CT (Computed Tomography) Equipament Nº CRCE-010. 2010. Disponível em: https://www.gov.uk/government/uploads/system/uploads/attachment_data/file/340159/HPA-CRCE-010_for_website.pdf
15. Ludlow JB, Davies-Ludlow LE, Brooks SL. Dosimetry of two extraoral direct digital imaging debices: NewTom cone beam CT and Orthophos Plus DS panoramic unit. Dentomaxillofac Radiol. 2003; 32: 229-34.
16. Mah JK, Danforth RA, Bumann A, Hatcher D. Radiation absorbed in maxillofacial imaging with a new dental computed tomography device. Oral Surg Oral Med Oral Pathol Oral Radiol Endod. 2003; 96: 508-13.
17. Tsiklakis K, Donta C, Gavala S, Karayianni K, Kamenopoulou V, Hourdakis CJ. Dose reduction in maxillofacial imaging using low dose Cone Beam CT. Eur J Radiol. 2005; 56: 413-17.

18. Ludlow JB, Ivanovic M. Comparative dosimetry of dental CBCT devices and 64-slice CT for oral and maxillofacial radiology. Oral surg. oral med. oral pathol. oral radiol. endod. 2008; 106: 106-14.

19. Chau ACM, Fung K. Comparison of radiation dose for implant imaging using conventional spiral tomography, computed tomography, and cone-beam computed tomography. Oral surg. oral med. oral pathol. oral radiol. endod. 2009; 107:.559-65.

20. Loubele M, Bogaerts R, Van Dijck E, Pauwels R, Vanheusden S, Suetens P, et al. Comparison between effective radiation dose of CBCT and MSCT scanners for dentomaxillofacial applications. Eur J Radiol. 2009; 71: 461-8.

21. Qu XM, Gang L, Ludlow JB, Zhang Z, Ma X. Effective radiation dose of ProMax 3D cone-beam computerized tomography scanner with different dental protocols. Oral Surg Oral Med Oral Pathol Oral Radiol Endod. 2010; 110: 770-6.

22. Davies J, Johson B, Drage NA. Effective doses from cone beam CT investigation of the jaws. Dentomaxillofac Radiol. 2012; 41: 30-6.

23. Pauwels R, Beinsbergera J, Collaertb B, Theodorakouc C, Rogerse J, Walkerc A et al. Effective dose range for dental cone beam computed tomography scanners. Eur J Radiol. 2012; 81: 267-71.

24. Soares MR, Batista WO, Antônio PL, Caldas LVE, Maia AF. Study of effective dose of various protocols in equipment cone beam CT. Appl Rad Isotop. 2015; 100: 21-6.

25. Abduwani JAA, Zilinskiene L, Colley S, Ahmed S. Cone beam CT paranasal sinuses versus standard multidetector an d low dose multidetector CT studies. Am J Otolaryngol. 2016; 37: 59-64.

26. Zenóbio EG, Zenóbio MAF, Nogueira MS, Silva TA, Shibli JA. Absorbed Radiation Doses During Tomographic Examination. Clin Implant Dent. Relat Res. 2012; 14:366-72.

27. Kadesjö N, Benchimol D, Falahat B, Näsström K, Shi XQ. Evaluation of the effective dose of cone beam CT and multislice CT for temporomandibular joint examinations at optimized exposure levels. Dentomaxillofac Radiol. 2015; 2: 20150041.

28. Shin HS, Nam KC, Park H, Choi HU, Kim HY, Park CS. Effective doses from panoramic radiography and CBCT (cone beam CT) using dose area product (DAP) in dentistry. Dentomaxillofac Radiol. 2014; 43: 20130439.

29. Lukat TD, Wong JCM, Lam EWN. Small field of view cone beam CT temporomandibular joint imaging dosimetry. Dentomaxillofac Radiol. 2013; 42: 20130082.

30. Al-Okshi A, NilssonM, Petersson A, WieseM, Lindh C. Using GafChromic film to estimate the effective dose from dental cone beam CT and panoramic radiography. Dentomaxillofac Radiol. 2013; 42: 20120343.

31. Okano K, Ayako M, Goto K, Yokoi M, Hirukawa A, Okumura S et al. Comparison of Absorbed and Effective Dose from Two Dental Cone Beam Computed Tomography Scanners Japa J Radiol Techn. 2012; 68: 216-25.

32. Librizzi ZT, Tadinada AS, Valiyaparambil JV, Lurie AG, Mallya SM. Cone-beam computed tomography to detect erosions of the temporomandibular joint: effect of field of view and voxel size on diagnostic efficacy and effective dose. Am J Orthod Dentofacial Orthop. 2011; 140: e25-30.

4.2 Artigo 2

Determinação da dose de radiação e risco radioinduzido de câncer em exames tomográficos cone beam para a avaliação da atm.

Artigo será submetido à **Dentomaxillofacial Radiology** (Qualis A1)**,** cujas normas para submissão de artigos podem ser visualizadas no endereço eletrônico: http://www.birpublications.org/page/ifa/bjr.

Determinação das doses de radiação e risco radioinduzido de câncer em exames tomográficos de feixe cônico para a avaliação da ATM

Determination of radioinduced radiation doses and risk of cancer in conical beam tomography examinations for the assessment of TMJ

C D B Azevedo[1]; M A F Zenóbio[2]; F R Manzi[3]; M S Nogueira[3]; E G Zenóbio[3*]

[1]Programa de Pós-graduação em Odontologia - Mestrado em Clínicas Odontológicas da Pontifícia Universidade Católica de Minas Gerais, Belo Horizonte, MG, Brasil; [2]Centro de Desenvolvimento da Tecnologia Nuclear-CDTN/CNEN, Belo Horizonte, MG, Brasil; [3]Departamento de Odontologia da Pontifícia Universidade Católica de Minas Gerais, Belo Horizonte, MG, Brasil.

*Correspondência para o autor:

- Dr. Élton Gonçalves Zenóbio - Av. Dom José Gaspar, Prédio 46 - Programa de Pós-graduação em Odontologia, Coração Eucarístico, Belo Horizonte - MG - CEP: 30535-901 - Telefone: 55 31 33194414 - zenóbio@pucminas.br

RESUMO

Objetivo: Este estudo avaliou os valores de dose na superfície de entrada na pele, dose equivalente, dose efetiva, assim como o risco radioinduzido de câncer e alterações morfofuncionais, calculados de acordo com o BEIR VII (2006) nos órgãos e tecidos radiossensíveis. A avaliação total da articulação temporomandibular (ATM) por meio da tomografia computadorizada de feixe cônico (TCFC) – (tomógrafo Kodak 9000C 3D®) foi o exame avaliado.

Material e métodos: Dosímetros termoluminescentes de Lif (TL-100H) foram posicionados em um simulador antropomórfico Alderson RANDO do modelo feminino, em locais correspondentes: cérebro, cortical óssea, cristalino, glândulas salivares, mucosa oral, linfonodos cervicais, tireoide, esôfago, região extratorácica, medula óssea, pulmões, mamas, fígado, estomago, cólon, ovários, útero e bexiga. Os dosímetros foram analisados pela leitora Harshaw 5500 Thermo Eléctron® conectada a um computador com o software Win-REMS®

Resultados: As maiores doses equivalentes detectadas foram de 12,475mGy nas glândulas parótidas; 1,086mGy no cristalino e 0,753mGy no cérebro; As menores doses foram para as regiões abaixo da medula óssea (osso esterno) anatomicamente com dose <0,007mGy. O valor da dose efetiva foi de 0,4709mSv. De acordo com os cálculos baseados no BEIR VII, os órgãos que apresentaram maiores riscos radioinduzido de câncer e alterações morfofuncionais são as glândulas salivares, cristalino e cérebro.

Conclusão: As regiões das glândulas parótidas, cristalino e cérebro, obtiveram os maiores valores de dose equivalente e risco radioinduzido de câncer e alterações morfofuncionais durante o exame TCFC para avaliação da ATM. Os dados obtidos no presente estudo sugerem novas pesquisas para obtenção dos valores de dose em diferentes tomógrafos e medidas de proteção, além de estudos para a otimização da dose de radiação no exame de TCFC, com o intuito de reduzir ao mínimo possível a exposição à radiação durante o exame assim como a radiação secundária e a perda da qualidade de imagem.

Palavras-chave: Articulação temporomandibular; Tomografia computadorizada de feixe cônico; Dose de radiação; Dosimetria termoluminescente.

ABSTRACT

Objective: This study evaluated the values of entrance surface doses, equivalent dose, effective dose, as well as the risk of cancer and morphofunctional changes calculated according to BEIR VII (2006) in Radiosensitive organs and tissues. The total evaluation of temporomandibular joint (TMJ) by concomitant computed tomography (CBCT) - (Kodak 9000C 3D® tomograph) was the exam evaluated.

Materials and methods: Lifting (TL-100H) thermoluminescent dosimeters were placed in an Alderson RANDO anthropomorphic simulator of the female model, in corresponding places: brain, cortical bone, lens, salivary glands, oral mucosa, cervical lymph nodes, thyroid, esophagus, region Extrathoracic, bone marrow, lungs, breasts, liver, stomach, colon, ovaries, uterus and bladder. The dosimeters were analyzed by the Harshaw 5500 Thermo Electron® reader connected to a computer with Win-REMS® software

Results: The highest equivalent doses detected were 12,475mGy in the parotid glands; 1,086mGy in the lens and 0,753mGy in the brain; The lowest doses were for the regions below the bone marrow (sternal bone) anatomically with dose <0,007mGy. The effective dose value was 0,4709 mSv. According to the calculations based on the BEIR VII, the organs that presented the greatest risk of cancer and morphofunctional changes are the salivary glands, lens and brain.

Conclusion: The regions of the parotid glands, lens and brain, obtained the highest values of equivalent dose and radio-induced risk of cancer and morphofunctional changes during the CBCT examination for TMJ evaluation. The data obtained in the present study suggest new research to obtain the dose values in different tomographs and protective measures, as well as studies for the optimization of the radiation dose in the CBCT examination, in order to minimize the exposure to radiation During the examination as well as secondary radiation and loss of image quality.

Keywords: Temporomandibular joint; Cone-beam computed tomography; Radiation dose; Thermoluminescent dosimetry

Introduction

The concern with the radioprotection of the patient is an increasingly studied reality, taking into account the principles of justification and optimization (ALARA) of the radiation dose[1-4]. In order to obtain a measurement standard, especially in the tomography examination (CBCT), considered a recent modality, since its first equipment was introduced in the 1990s[2,5], international norms and guidelines related to CBCT are disclosed, with the objective of raising awareness among operators and professionals in the health area[2,6,7]. However, despite the relevant studies found in the literature[8-18], there are still few data related to the radiation dose in CBCT in the examination for the evaluation of the TMJ[19-21].

The temporomandibular joint is a biaxial joint, classified as the most complex joint of the human body. It is the junction of the mandibular bone to the skull. Among its functions, the most important are chewing and phonation[22] deserving special attention from health professionals, since it can be affected by pathological conditions and disorders that also affect the other joints of the organism. Therefore, for evaluation, diagnosis and planning, more sensitive imaging tests are necessary, with magnetic resonance imaging being the most appropriate examination for evaluation of soft tissues and computed tomography for evaluation of hard tissues of the TMJ structures[23,24].

Because it represents an emerging technology, which allows high volumetric resolution, scanning of the structures in the sagittal, coronal, and axial planes, the CBCT is almost totally free of overlaps. It presents lower dose of radiation to the patient and lower cost, when compared to the TC Multislice (MSCT). Thus, CBCT began to be increasingly used for bone evaluation of TMJ[5,25,26].

In order to obtain radiation dose values during CFCT exams, several investigators[8-14,16-18] carried out studies using an anthropomorphic simulator with thermoluminescent dosimeters positioned in places referring to organs considered radiosensitive, for measurement and calculation of radiation doses, and (NRDs) for this modality of examination not mentioned in the European Commission 2014. The knowledge of the doses of radiation in CBCT is of great importance because of the lack of uniformity in the configuration of the equipment, with Different fields of view (FOV) and equipment rotating at 180, 210 and 360 degrees[27].

In this context, this study evaluated the entrance surface dose, equivalent dose of organs and tissues, effective dose and radiation risk of cancer and morphofunctional changes in organs and tissues during a total TMJ examination using CBCT, Kodak 9000C 3D scanner, using the thermoluminescent dosimetry method.

Material and methods

This experimental quantitative study was developed in the laboratories of the Center for the Development of Nuclear Technology (CDTN / CNEN) and Radius Odonto Clinic, Belo Horizonte, Brazil.

The absorbed dose and the entrance surface dose values were obtained by means of 95 LiF thermoluminescent dosimeters (TL-100H, Harshaw-Bricon), 4 separate dosimeters for obtaining the background radiation dose (BackGround). All were selected according to physical criterion inspection, uniformity and reproducibility and lower limit of detection according to ISO 12794, 2000. All dosimeters were numbered and were able to receive the energy levels of the photons used in the Kodak 9000C 3D, and allow reading using the Harshaw 5500 reader (Thermo Electron Corporation) with the RPM-Bricon WinREMSTM software coupled.

Like the studies already cited[8-14,16-18], the dosimeters were positioned in the Alderson RANDO (Alderson Research Laboratories, Stanford, CT) anthropomorphic simulator. In the present study, the model used was the female model, with 600ml of the breast representing a standard adult woman, with dimensions of approximately 1.55m in height, 50kg mass without arms and legs (Figure 1).

The chosen organs and tissues are considered to be sensitive to radiation[4,28]. The corresponding region of each organ was positioned according to the anatomy atlas of Sobotta (Table 1).[29]

Table 1- Positioning of the TL-100H in the Alderson RANDO simulator

Anatomical points	Slice Simulador
Brain (right and left)	3
Cortical bone (right and left)	3
Lens (right and left)	3
Parotid Gland (right and left)	5
Submandibular and Sublingual Gland (right and left)	6
Oral Mucosa (right and left)	6
Cervical Lymph Node (right and left)	8
Thyroid (right and left)	9
Esophagus	13
Parasternal region (right and left)	13
Bone marrow	14
Lung (right and left)	14
Mama (right and left)	16
Liver	18
Stomach	19
Colon (right and left)	24
Ovary (right and left)	29
Uterus	30
Bladder	30

Figure 1- Anthromorphic Alderson RANDO simulator

The positioning of the female RANDO simulator on the Kodak 9000C 3D tomograph was through the imaging sensor of the equipment itself, being initially positioned with the median sagittal plane parallel to the rotational center of the conical beam equipment to align the anthropomorphic simulator to the region of interest of the TMJ. In all the acquisitions the simulator obtained the same vertical and horizontal positioning.

The Kodak 9000C 3D acquisitions were performed using the following parameters (Table 2).

Table 2- Kodak 9000C 3D CBCT image acquisition parameters

Tube tension	70 kV
Tube current	10 mA
Exposure time (rotation)	10,8 seconds
FOV	5,0cm x 3,7cm
Isotropic Voxel Size	76x76x76μm^3
Target Angle	5º
Inherent Filtration	2,5mmAl
Distance focus-detector	60cm

The protocol used for the examination of each TMJ, are two tomographic acquisitions, one with the mouth open and the other closed; Totaling 4 acquisitions for the bilateral evaluation.

Five total examinations for TMJ were performed (20 acquisitions), with TL-100H being replaced at each examination, in order to obtain a more accurate average value of the doses in the organs and tissues.

In order to obtain the values of absorbed doses of organs and tissues, the reports of ICRP 103[4], and studies[9,11,13] were obtained as a base, using the following formula:

$$\mathrm{D_T} = D.\left(\frac{\mu en}{\rho}\right)_{tissue/air}$$

Where *D* is the mean value of the readings of the dosimeters in mGy, and *μen/ρ tissue/air* is the ratio between the mass energy absorption coefficients of the tissues and air for the average energy of the test qualities.

By means of the elemental constitution of each organ of interest and the air[30,31] are presented in Table 3, using the Online Program XCOM (National Institute of Standards and

Technology - NIST) to obtain the coefficient of mass energy absorption of tissues and air, taking as reference the average energy Of the Kodak 9000C 3D device (0.368 MeV) calculated by the XCOMP5R program[32].

The equivalent dose is the mean value of the absorbed dose (DT, R) in a tissue or organ (T), obtained over the whole tissue or organ (T), due to the radiation (R), taking into account the radiation factor WR), as demonstrated in formula:

$$H_T = \sum_R W_R \cdot D_{T,R}$$

As the X-ray radiation factor is equal to 1, the values of the absorbed dose will be the same as the respective equivalent dose for each organ or tissue, but instead of mGy, the unit of the equivalent dose is mSv.

The effective dose was calculated according to the recommendations of the ICRP 103 (2007) and the tissue weighting factors (W_T).

$$E = \sum_T W_T \cdot H_T$$

Where *E* is the weighted sum of equivalent doses in all tissues or organs of the body in which W_T is the weight factor for tissue T and H_T is the dose equivalent to the respective tissue.

In order to calculate the estimate of the radio-induced risk of cancer and morphofunctional changes, the report of the Biologic Effects of Ionizing Radiation (BEIR VII) 3 of the year 2006 was used.

The BEIR VII report(2006)[3] considers the sex and age of the exposure, being the greater risk for the female sex and in younger individuals. The formula used for the calculation is:

$$R = r_T \,.\, H_T$$

Where: R comprises the actual risk of cancer incidence, rT is the cancer risk specific to the tissue or organ and H_T which is the equivalent dose in tissue T.

Table 3: Elemental composition of tissues and organs of the body (% by mass)

Site	**H**	**C**	**N**	**O**	**Na**	**Mg**	**P**	**S**	**Cl**	**Ar**	**K**	**Ca**	**Fe**	**I**
Air		<0.001	0.755	0.231						0.012				
Soft tissue*	0.106	0.315	0.024	0.547	0.001		0.002	0.003	0.002		0.002			
Thyroid	0.104	0.119	0.024	0.745	0.002		0.001	0.001	0.002		0.001			0.001
Gastro.Tract **	0.100	0.222	0.022	0.644	0.001		0.002	0.003	0.001		0.004	0.001		
Salivary gl.***	0.105	0.100	0.023	0.763	0.002		0.001	0.002	0.002		0.002			
Cortical boné	0.034	0.1550	0.042	0.435	0.001	0.002	0.103	0.003	X			0.225		
Brain	0.107	0.145	0.022	0.712	0.002		0.004	0.002	0.003		0.003			
Mama	0.106	0.332	0.030	0.527	0.001		0.001	0.002	0.001					
Lens	0.096	0.195	0.057	0.646	0.001		0.001	0.003	0.001					
Lung	0.103	0.105	0.031	0.749	0.002		0.002	0.003	0.003		0.002			
Ovary	0.105	0.093	0.024	0.768	0.002		0.002	0.002	0.002		0.002			
Uterus	0.102	0.143	0.034	0.710	0.001		0.002	0.003	0.001		0.004			
Bone marrow	0.105	0.414	0.034	0.439			0.001	0.002	0.002		0.002		0.001	

*Female soft tissues (skin, bone marrow, liver, brain, intestine, lung, lymph, bladder, thyroid, uterus)
**Gastrointestinal Tract
***Salivary glands

Results

The entrance surface doses of each organ and tissue was calculated by means of the average of the doses obtained in the five examinations. The highest values were obtained in the corresponding regions of the parotid glands, the lens and submandibular and sublingual glands, being larger on the left side when compared to the right side. The lowest values were for the parasternal regions and anatomically below them, as evidenced in table 4.

Tabela 4- The entrance surface doses (ESD) values during TMJ examination in CBCT (mGy)

Anatomical points	ESD (mGy)
Lens (right)	0,756±0,12
Lens (left)	1,036±0,23
Parotid Gland (right)	9,377±0,82
Parotid gland (left)	19,161±1,26
Submandibular and Sublingual Gland (right)	0,677±0,13
Submandibular and Sublingual Gland (left)	1,001±0,24
Oral mucosa (right)	0,589±0,17
Oral mucosa (left)	0,661±0,15
Cervical lymph node (right)	0,131±0,05
Cervical lymph node (left)	0,271±0,05
Thyroid	0,082±0,01
Parasternal region (right)	0,049±0,01
Parasternal region (left)	0,166±0,06
Others*	<0,007±0,01**

*Others correspond to organs and tissues: Breast (right and left); Lung (right and left); Liver; Stomach; Colon (right and left); Ovary (right and left); Uterus; Bladder;

** The value detected by the dosimeters was below the lower limit of detection.

In order to calculate the absorbed dose it was necessary to obtain the mass energy absorption coefficients of tissues and air for the energy range 0.0368 MeV of the KODAK 9000C 3D tomograph. The results are shown in table 5.

Table 5- Mass and tissue energy absorption coefficients for the 0.0368 MeV energy range of the KODAK 9000C 3D tomograph (cm²/g)

Sites	XCOM (cm²/g)
Air	0,2372
Brain	0,7394
Lens	0,2615
Bone marrow (sternum)	0,2426
Thyroid	0,2487
Cortical boné	0,2609
Salivary glands	0,2600
Esophagus	0,2493
Feminine soft tissue	0,2591
Mamas	0,2462
Lung	0,2821
Skeletal muscle	0,2576
Ovary	0,2596
Colon	0,2576

Table 6 shows the values of the equivalent dose calculated according to the ICRP 1034 report. As with the absorbed dose, the highest equivalent doses were the parotid gland region, followed by the regions corresponding to the lens and brain.

Table 6- Equivalent dose values in tissues during TMJ examination in CBCT

Anatomical points	H_T (mSv)
Brain	0,753
Cortical boné	0,127
Lens	1,086
Parotid Gland	12,475
Submandibular and Sublingual Gland	0,560
Oral mucosa	0,644
Cervical Lymph Node	0,372
Thyroid	0,235
Esophagus	0,047
Parasternal Region	0,038
Bone marrow	0,021
Others*	<0,007**

*Others correspond to organs and tissues: Breast; Lung; Liver; Stomach; Colon; Ovary; Uterus; Bladder;

**The value detected by the dosimeters was below the lower limit of detection.

The ICRP 103 (2007)[4] was used to calculate the effective dose. The result obtained was 0.4709mSv.

The Table 7 presents the estimation of the risk of radio-induced cancer and morphofunctional changes by the BEIR VII[3]. As can be notes in the values obtained in BEIR VII, the risk decreases with increasing age, the organs of the salivary glands, lens and brain.

Table 7- Estimation of the risk of radio-induced cancer and morphofunctional changes according to BEIR VII (among 100,000 people exposed to 0.1Gy).

	BEIR VII						
Anatomical points	20	30	40	50	60	70	80
Thyroid	0,265	0,096	0,033	0,009	0,002	<0,001	0
Cervical Lymph Node	1,201	0,769	0,673	0,550	0,405	0,252	0,111
Oral mucosa	2,081	1,333	1,166	0,953	0,702	0,438	0,193
Parasternal Region	0,123	0,079	0,069	0,056	0,041	0,026	0,011
Bone marrow	0,015	0,013	0,013	0,013	0,012	0,010	0,008
Mama	0,036	0,021	0,012	0,006	0,002	0,001	<0,001
Lung	0,024	0,017	0,017	0,016	0,014	0,010	0,005
Liver	0,001	<0,001	<0,001	<0,001	<0,001	<0,001	<0,001
Stomach	0,002	0,001	0,001	0,001	0,001	<0,001	<0,001
Colon	0,017	0,012	0,012	0,010	0,009	0,006	0,003
Ovary	0,005	0,003	0,003	0,002	0,001	0,001	<0,001
Uterus	0,001	<0,001	<0,001	<0,001	<0,001	<0,001	<0,001
Bladder	0,001	<0,001	<0,001	<0,001	<0,001	<0,001	<0,001
Salivary glands	40,293	25,822	22,579	18,462	13,597	8,482	3,742
Brain	2,432	1,558	1,362	1,113	0,820	0,511	0,225
Lens	3,508	2,248	1,966	1,607	1,183	0,738	0,325
Cortical bone	0,409	0,262	0,229	0,187	0,138	0,086	0,038
Esophagus	0,152	0,097	0,085	0,069	0,051	0,032	0,014

Discussion

The equivalent dose of the patient's organs can be used for assessing the risk of cancer, such as the 2006 BEIR VII report, which was based on long-term epidemiological studies of cancer induction in the population affected by the disease. Two nuclear bomb explosions in Japan in 1945. Its risk model is the linear (LNT) linear model that provides the most reasonable description of the relationship between low dose exposure of ionizing radiation and the incidence of cancers Solids that are induced by ionizing radiation, except for leukemia, which the committee adopted the linear-quadratic model. This estimate of the radiation-induced risk of cancer considers the sex and age of the patient at exposure, being the greatest risk for the female sex and for exposure in younger individuals. The result obtained is the number of cases per 100.000 people exposed by a dose of 0,1 Gy[3]. According to the calculation of BEIR VII, the organs with the highest risk in the CBCT examination in the TMJ evaluation are: salivary glands, lens and brain.

The effective dose is useful for comparing radiation doses in different diagnostic procedures and comparing the use of similar technologies and procedures in different hospitals and countries4. In the present study the effective dose was 470,9µSv for the whole body. In the Librizzi et al[19] and Lukat et al[20], Performed the dosimetry study with TLDs positioned in an anthropomorphic simulator during a CBCT examination for TMJ evaluation and obtained 558µSv and 223,6 ± 1.1µSv, respectively, as can be seen in table 8. By the difference of tomographs and parameters used between studies, justifies the difference in effective dose values between them.

Table 8- Effective dose during a bilateral examination for TMJ evaluation

	***E* (µSv)**	**CBCT**	**Exam Parameters**
Present study	470,9	Kodak 9000C 3D	70kV, 108mAs
Librizzi et al.[19]	558	Hitachi CB Mercuray	120kV e 150 mAs
Lukat et al.[20]	223,6±1,1	Hitachi CB Mercuray	100kV, 96mAs

Studies[8-18] used an anthropomorphic simulator with thermoluminescent dosimeters placed in regions corresponding to the radiosensitive organs for the measurement of radiation doses during CBCT exams. This methodology suggests the obtaining of more reliable measures in relation to studies in patients justifying its use in the present study.

Radiation-sensitive organs and tissues were selected according to the documents[3,4], combined with the respective calculations for the doses of radiation and radiation-induced risk of cancer and morphofunctional changes.

The thyroid gland should be taken into account, due to the fact that it is an organ with high sensitivity and risk of cancer, especially in childhood[33]. The data from the present study showed that the thyroid gland was not the one that obtained the highest equivalent dose value with a value of 0,235mSv. In the study of Lukat et al.[20] The equivalente dose of 0,0189mSv in the Hitachi CBCT, using 100kV and 10mA, and 0,00187mSv in the Kodak 9000 3D tomograph, using 70kVp, 10mA and 10,8 seconds, were obtained. In Librizzi et al[19] obtained the result of 0,001075mSv in a FOV 6-in in the CBCT Hitachi CB Mercuray, with parameters of 120kV and 150mAs. In addition to the parameters, the technique in their studies were different, which would explain the difference in radiation dose values between the studies.

Due to the proximity of the region corresponding to the parotid gland with the TMJ region, it is expected to obtain a higher radiation dose value during the examination, since the FOV positioned in the TMJ is very close to this gland. Studies with CBCT in examinations of the dentomaxillofacial region have shown that the salivary gland was the organ most exposed to radiation, even though the tissue weighting factor of the effective dose of the thyroid is 4 times higher than the salivary glands[10,11,20,21,34]. In the present study, the salivary glands were the ones that had the highest radiolabeled risk of cancer and morfunctions during the total TMJ examination. For measurement, the measurement of the parotid glands, the submandibular and sublingual glands was separated, due to the anatomical positioning. However, due to the anatomical proximity of the submandibular and lingual gland, the radiation dose was measured at a midpoint. The parotid glands obtained the values of 12,475mSv of equivalent dose. The submandibular and sublingual glands were 0,560 mSv. During the calculations of the present study, it was notes that the left side obtained a higher dose of radiation than the right side. By evaluating the operation of the Kodak 9000C 3D tomography device, during the TMJ examination, it was notes that it begins and ends with a greater slope to the left side of the patient. It is suggested that due to this inclination, because of the lack of initiation and termination of tomographic acquisition in the middle of the patient's medial sagittal plane, this difference in dose values between the sides occurs. In the study of Chau e Fung[12] On dosimetry in CBCT, we find similar findings to the present study. The authors reported that the source was closer to one side, as in the present study, justifying the differences found between the left and right sides of the organs measured. In the study of Lukat et al.[20], in the Hitachi apparatus they obtained 0,03673mSv for the salivary glands and 0,00383mSv in the Kodak 9000 3D. The Hitachi CBCT exposure parameters were 100kVp and 10mA and in the Kodak 9000 3D CBCT of 70kVp and 10mA. In the study of Librizzi et al.[19] obtained the value of 0,00962mSv in the CBCT Hitachi CB Mercuray, with parameters of 120kV and 150mAs. In addition to the parameters, the technique in their studies were different, which would explain the difference in radiation dose values between the studies.

Another issue of concern in the area of radioprotection is the lens. The lens was known to be a radiosensitive tissue, but current research suggests that its radiosensitivity is greater than previously thought[33]. The International Commission on Radiological Protection (ICRP) in 2012 revised the epidemiological evidence for cataracts and suggested that the value of the maximum radiation dose to be received in the tissue should be less than 0,5Gy instead of

2,0Gy and the exposure limit Occupational change from 150mSv to 20mSv per year[35,36]. This suggestion has already been made in the European Union and is being considered in the rest of the world. Oliveira et al.[36] performed a lens dosimetry study during an TMJ examination in CBCT, and obtained values of 5,4mSv, 5,8mSv, and 7,9mSv of equivalent dose for the lens on the Gendex GXCB 500 (Gendex Dental Systems, Pennsylvania, USA), CS 9000 (Carestream Health, New York, New York) and classic i-CAT (Imaging International Sciences, Hatfield, Pennsylvania, USA), respectively. Comparing with the present study that obtained a value of 1,086mSv of equivalent dose for the organ of the lens, being the second organ with the highest risk of cancer and morphofunctional changes. The exposure parameters of the iCAT CBCT in the study by Oliveira et al.[36] Was 120kVp, 36mAs and in the Gendex CBCT was 120kVp and 30mAs which would explain the difference in radiation dose values between the studies. In a Ainsbury et al.[37] Presented a literature review with recently published information on the biological and mechanical aspects of cataract induced by exposure to ionizing radiation, with the main focus being the biological effects of low linear energy transfer of ionizing radiation. Dosimetry issues and a number of other confounders were also considered. The authors suggest a more complete understanding of lens exposure at relatively low doses of ionizing radiation to obtain prevention, protection and even treatment in case of ionizing radiation-induced cataracts. Due to the high radiosensitivity from organ, it is suggested that more dosimetric studies of the same be done.

The region corresponding to the brain in the present study obtained a value of 0,756mSv of equivalent dose, being the third organ with the highest risk of cancer induced and morphofunctional changes. In the study of Lukat et al[20] the obtained value for this organ was 0,00242mSv and that of Librizzi et al.[19] The value was 0,013mSv. In the study of Lukat et al[20], The brain region was measured in slice 2 of the phantom, while the present study positioned the TLDs in the third slice of the phantom, being closer to the TMJ region, justifying the finding of a larger equivalent dose. When compared to the values obtained by Librizzi et al.[19], The difference between the tomographers and exposure parameters for the examination, justify the difference.

The smal FOV CBCT is indicated for local exams, with FOV being better suited for generic exams or in larger regions such as orthodontic treatment planning, orthognathic surgical planning, bridging or denture assembly, and trauma cases.

The present study used a smaller FOV tomograph measuring 5.0cm x 3.7cm, and it was necessary to obtain 4 tomographic acquisitions to obtain open and closed images on both sides. In the study of Chau e Fung[12], The Scanora unit with a FOV of 4 cm by 4 cm produced lower doses when compared to other FOV scans larger, but when performing examinations in molars, the region of the parotid glands were inside the FOV, leading them to receive a higher dose During the CBCT examination, which would explain the dose values in the region of the parotid glands being the ones with the highest value in our study.

In CBCT, the lower the FOV used, the lower the patient's exposure to radiation in radiosensitive organs, since it prevents them from being inside the direct beam. Therefore, it is imperative that operators correctly use the examination protocols to provide images that respond to a diagnosis with the least amount of radiation possible.[12,38]

Chau e Fung[12] when comparing different tomographs, obtained a lower radiation dose in the FOV (Scanora) compared to FOV (iCAT). However, in the study by Oliveira et al 2015, when comparing dose values of Gendex GXCB 500 CBCT with FOV and greater stress, presented doses similar to CS9000. Thus, although CS 9000 has FOV fixed and smaller than the Gendex GXCB 500, it did not result in reduced radiation doses. This shows that studies on this issue should continue.

Conclusion

The parotid glands obtained the highest equivalent dose value during the total CBCT examination due to their anatomical location, proximity to FOV and the technique performed, presenting the highest risk of cancer and morphofunctional changes, followed by the lens and brain .

The lens was the second organ with the highest equivalent dose value. Because it is a more radiosensitive organ than was believed, it is suggested that more studies are carried out with the intention of reducing the dose of radiation or to obtain a mechanism of protection for the same.

Research on dosimetry in patients involves variables such as parameters of exposure, positioning and methodology, which suggests the need for new studies on dosimetry in CBCT of the dentomaxillofacial regions, with the objective of optimizing the radiation dose in patients with adequate image quality for Diagnosis and determination of diagnostic reference levels.

REFERENCES

1. United Nations Scientific Committee on the Effects of Atomic Radiation. Sources and effects of ionizing radiation. Unscear 2000 report to the general assembly, volume 1. 2000. Disponível em: http://www.unscear.org/docs/publications/2000/UNSCEAR_2000_Report_Vol.I.pdf.
2. European Commission. Radiation protection safety and efficacy of a new and emerging dental X-ray modality (SEDENTEXCT). Project final report, 2012. Disponível em: http://www.sedentexct.eu/files/radiation_protection_172.pdf.
3. National Research Council. Health risks from exposure to low levels of ionizing radiation: BEIR VII phase 2. Washington, USA: The Nacional Academy of Sciences. USA, 2006.
4. International Commission the Radiological Protection. Recommendations of the international commission on radiological protection. In: Annals of the ICRP. Oxford: Pergamon Press, 2007, v.37, n.2-4, ICRP 103.
5. Rehani MM. Radiological protection in computed tomography and cone beam computed tomography. 2015; **44:** 229-235.
6. International Atomic Energy Agency. Human Health Reports Nº5: Status of computed tomography dosimetry for wide cone beam scanners. Viena: IAEA, 2011. Disponível em: http://www.iaea.org/Publications/index.html.
7. Health Protection Agency. Working Party on Dental Cone Beam CT Equipament: Guidance on the Safe Use of Dental Cone Beam CT (Computed Tomography) Equipament Nº CRCE-010, 2010. Disponível em: https://www.gov.uk/government/uploads/system/uploads/attachment_data/file/340159/HPA-CRCE-010_for_website.pdf.
8. Ludlow JB, Davies-Ludlow LE, Brooks SL. Dosimetry of two extraoral direct digital imaging debices: NewTom cone beam CT and Orthophos Plus DS panoramic unit. Dentomaxillofac Radiol 2003; **32:** 229-234.
9. Mah JK, Danforth RA, Bumann A, Hatcher D. Radiation absorbed in maxillofacial imaging with a new dental computed tomography device. Oral Surg Oral Med Oral Pathol Oral Radiol Endod 2003; **96:** 508-513.
10. Tsiklakis K, Donta C, Gavala S, Karayianni K, Kamenopoulou V, Hourdakis CJ. Dose reduction in maxillofacial imaging using low dose Cone Beam CT. Eur J Radiol 2005; **56:** 413-417.

11. Ludlow JB, Ivanovic M. Comparative dosimetry of dental CBCT devices and 64-slice CT for oral and maxillofacial radiology. Oral Surg Oral Med Oral Pathol Oral Radiol Endod 2008; **106:** 106-114.
12. Chau ACM, Fung K. Comparison of radiation dose for implant imaging using conventional spiral tomography, computed tomography, and cone-beam computed tomography. Oral Surg Oral Med Oral Pathol Oral Radiol Endod 2009; **107:** 559-565.
13. Loubele M, Bogaerts R, Van Dijck E, Pauwels R, Vanheusden S, Suetens P, et al. Comparison between effective radiation dose of CBCT and MSCT scanners for dentomaxillofacial applications. Eur J Radiol 2009; **71:** 461-468.
14. Qu XM, Gang L, Ludlow JB, Zhang Z, Ma X. Effective radiation dose of ProMax 3D cone-beam computerized tomography scanner with different dental protocols. Oral Surg Oral Med Oral Pathol Oral Radiol Endod 2010; **110:** 770-776.
15. Davies J, Johson B, Drage NA. Effective doses from cone beam CT investigation of the jaws. Dentomaxillofac Radiol 2012; **41:** 30-36.
16. Pauwels R, Beinsberger J, Collaert B, Theodorakou C, Rogers J, Walker A, et al. Effective dose range for dental cone beam computed tomography scanners. Eur J Radiol 2012; **81:** 267-271.
17. Soares MR, Batista WO, Antônio PL, Caldas LVE, Maia AF. Study of effective dose of various protocols in equipment cone beam CT. Appl Rad Isotop 2015; **100:** 21-26.
18. Abduwani JAA, Zilinskiene L, Colley S, Ahmed S. Cone beam CT paranasal sinuses versus standard multidetector an d low dose multidetector CT studies. Am J Otolaryngol 2016; **37:** 59-64.
19. Librizzi ZT, Tadinada AS, Valiyaparambil JV, Lurie AG, Mallya SM. Cone-beam computed tomography to detect erosions of the temporomandibular joint: effect of field of view and voxel size on diagnostic efficacy and effective dose. Am J Orthod Dentofacial Orthop 2011l; **140:** e25-30.
20. Lukat TD, Wong JCM, Lam EWN. Small field of view cone beam CT temporomandibular joint imaging dosimetry. Dentomaxillofac Radiol, 2013; **42:** 20130082.
21. Kadesjö N, Benchimol D, Falahat B, Näsström K, Shi XQ. Evaluation of the effective dose of cone beam CT and multislice CT for temporomandibular joint examinations at optimized exposure levels. Dentomaxillofac Radiol, 2015; **2:** 20150041. [Epub ahead of print].

22. Alomar X, Medrano J, Cabratosa J, Clavero JA, Lorente M, Serra I, et al. Anatomy of the temporomandibular joint**.** Semin Ultrasound CT MRI 2007; **28:** 170-183.
23. Utumi ER, Perrella A, Albuquerque MAP, Adde CA, Rocha RG, Cavalcanti GP. Evaluation of simulated boné lesion in the head of the mandible by using multislice computed tomography. J Appl Oral Sci 2009; **17:** 21-26.
24. Barghan S, Tetradis S,Mallya SM. Application of cone beam computed tomography for assessment of the temporomandibular joints. Austr Dent J 2012; **57:** 109-118.
25. Scarf WC, Farman AG, Sukovic P. Clinical applications of cone-beam computed tomography in dental practice. J Can Dent Assoc 2006; **72:** 75-80.
26. Zhang ZL, Cheng JG, Li G, Shi XQ, Zhang JZ, Zhang ZY, et al. Detection accuracy of condylar bony defects in Promax 3D cone beam CT images scanned with different protocols. Dentomaxillofac Radiol 2013; **42:** 1-6.
27. Batista WO, Navarro MV, Maia AF. Development of a phantom and a methodology for evaluation of depth Kerma and Kerma Index for dental Cone Beam Computed Tomography. Radiat Prot Dosimetry. 2013; **157**: 543-551.
28. Morant JJ, Salvadó M, Hernández-Girón I, Cassanova R, Ortega R, Calzado A. Dosimetry of a cone beam CT device for oral and maxillofacial radiology using Monte Carlo techniques and ICRP adult reference computational phantoms. Dentomaxillofac Radiol 2013; **42:** 1-9.
29. Sobotta J. Atlas de anatomia humana sobotta: cabeça, pescoço e extremidade superior (21ª ed). Rio de Janeiro: Guanabara Koogan, 2000.
30. International Commission on Radiological Units and Measurements. Tissue substitute in radiation dosimetry and measurements.Bethesda: UCRU, 1998. 24p. (ICRU-44).
31. White DR, Woodard HQ, Hammond SM. Average soft-tissue and bone models for use in radiation dosimetry. The Brit J Radiol 1987, **60**: 907-913.
32. Nowotny R, Hofer A. Ein program fur die berechunung von diagnostischen ronttgenspektren Fortschr. Rontgenstr. 1985, **142:** 1309–18.
33. Ludlow JB, Davies-Ludlow LE, Brooks SL, Howerton WB. Dosimetry of 3 CBCT devices for oral and maxillofacial radiology: CB Mercuray, NewTom 3G and i-CAT. Dentomaxillofac Radiol 2006; **35:** 219-226.
34. Al-Okshi A, Nilsson M, Petersson A, Wiese M, Lindh C. Using Gafchromic film to estimate the effective dose from dental cone beam CT and panoramic radiography. Dentomaxillofac Radiol 2013; **42:** 20120343.

35. International Commission the Radiological Protection. Statement on tissue reactions and early and late effects of radiation in normal tissues and organs–threshold doses for tissue reactions in a radiation protection context. In: Annals of the ICRP 41, 2012; 1-2. ICRP 118.
36. Oliveira MVL, Ely M, Andrade A, Batista WO, Campos PSF. Skin doses on the lens for temporomandibular joint exam in cone beam computed tomography. Braz Arch Biol Technol 2015; **58:** 886-890.
37. Ainsbury EA, et al Ionizing radiation induced cataracts: Recent biological and mechanistic developments and perspectives for future research. Mutat Res 2016; **770** (pt B): 238-26.
38. Schilling R, Geibel MA. Assessment of the effective doses from two dental cone beam CT devices. Dentomaxillofac Radiol 2013; **42:** 1-5.

5 CONSIDERAÇÕES FINAIS

A metodologia avaliou doses absorvidas, doses da superfície de entrada, dose equivalente e risco radioinduzido de câncer em diversos órgãos do tomógrafo de feixe cônico Kodak 9000C 3D em um exame total de ATM, gerando dados que ainda não foram observados até o momento na literatura.

As glândulas parótidas, o cristalino e o cérebro foram os órgãos que obtiveram maiores valores de dose absorvida durante o exame total de ATM no presente estudo, devido sua localização anatômica e proximidade do FOV. Porém, as regiões correspondentes a mucosa oral, linfonodo cervical e tireoide obtiveram os maiores valores para risco radioinduzido de câncer e alterações morfuncionais.

Estudos e pesquisas sobre este tema, em pacientes, envolvem muitas variáveis além do exame que está sendo avaliado, o que sugere a necessidade de novos estudos sobre dosimetria em TCFC das regiões dentomaxillofaciais, com o objetivo de otimização da dose, diminuindo assim, a exposição de radiação ao paciente, a determinação de níveis de referência de diagnóstico e uma qualidade de imagem adequada para o diagnóstico.

REFERÊNCIAS

ALOMAR, X. et al. Anatomy of the temporomandibular joint**. Seminars in Ultrasound CT and MRI,** v.28, n.3, p. 170-183, June 2007.

CHAU, A.C.M.; FUNG, K. Comparison of radiation dose for implant imaging using conventional spiral tomography, computed tomography, and cone-beam computed tomography. **Oral Surgery, Oral Medicine, Oral Pathology, Oral Radiology and Endodontology,** v.107, n.4, p.559-565, Apr. 2009.

EUROPEAN COMMISSION. **Radiation protection safety and efficacy of a new and emerging dental X-ray modality (SEDENTEXCT)**. Project Final Report, 2012. Disponível em: <http://www.sedentexct.eu/files/radiation_protection_172.pdf>. Acesso em: 25 Aug. 2015

FELDKAMP, L.A.; DAVIS, L.C.; KRESS, J.W. Practical cone-beam algorithm. **Journal of the Optical Society of America A**. v.1, n.6, p. 612-619, 1994.

GARIB, D.G et al. Tomografia computadorizada de feixe cônico (Cone beam): entendendo este novo método de diagnóstico por imagem com promissora aplicabilidade na Ortodontia **Revista Dental Press de Ortodontia e Ortopedia Facial,** v.12, n.2, p. 139-156, Mar./Apr. 2007.

HARSHAW-BICRON. **Materials and assemblies for thermoluminescence dosimetry.** Ohio, USA: Saint-Gobain Industrial Ceramics, 1998.

INTERNATIONAL COMMISSION ON RADIOLOGICAL UNITS AND MEASUREMENTS. Tissue substitute in radiation dosimetry and measurements. **Bethesda**: ICRU, 1998. 24p. (ICRU-44).

INTERNATIONAL COMMISSION THE RADIOLOGICAL PROTECTION. Recommendations of the international commission on radiological protection. In: **Annals of ICRP.** Oxford: Pergamon Press, 1991, v.22, n.1/3, ICRP 60.

INTERNATIONAL COMMISSION THE RADIOLOGICAL PROTECTION. Recommendations of the international commission on radiological protection. In: **Annals of the ICRP.** Oxford: Pergamon Press, 2007, v.37, n.2-4, ICRP 103.

INTERNATIONAL STANDARD NUCLEAR ENERGY. **Radiation protection-individual thermoluminescence dosemeters for extremities and eyes.** Press. Servieire, 2000, n. 12794.

KUMAR, M. et al. Cone beam computed tomography - Know its secrets. **Journal of International Oral Health,** v.7, n.2, p. 64-68, Feb. 2015.

LUDLOW, J.B. et al. Dosimetry of 3 CBCT devices for oral and maxillofacial radiology: CB Mercuray, NewTom 3G and i-CAT. **Dentomaxillofacial Radiology,** v.35. p.219-226, 2006

LUDLOW, J.B; IVANOVIC, M. Comparative dosimetry of dental CBCT devices and 64-slice CT for oral and maxillofacial radiology. **Oral Surgery, Oral Medicine, Oral Pathology, Oral Radiology and Endodontics,** v. 106, p.106-114, July 2008.

MATSUSHIMA, L.C. **Determinação das curvas de isodose e confirmação do planejamento em Radioterapia de Intensidade Modulada- IMRT convencional empregado as técnicas de termoluminescência, luminescência opticamente estimulada e detectores semicondutores**. 2015. Dissertação (Doutorado em Ciências na área de Tecnologia Nuclear) – Instituto de Pesquisas Energéticas e Nucleares, Universidade de São Paulo, São Paulo.

MORANT, J.J. Dosimetry of a cone beam CT device for oral and maxillofacial radiology using Monte Carlo techniques and ICRP adult reference computational phantoms. **Dentomaxillofacial Radiology,** v.42, n.92555893, p. 1-9, 2013.

NATIONAL RESEARCH COUNCIL. Health risks from exposure to low levels of ionizing radiation: BEIR VII phase 2. Washington, USA: The Nacional Academy of Sciences, 2006.

NOWOTNY R.; HOFER A. Ein program fur die berechunung von diagnostischen ronttgenspektren. **Fortschr Rontgenstr**, v.142, n.1, p.1309–1318, 1985.

PAUWELS, R. et al. Effective dose range for dental cone beam computed tomography scanners. **European Journal of Radiology,** v.81, n.2, p. 267-271, Feb. 2012.

RAMOS, A.C.A. et al. Articulação temporomandibular-aspectos normais e deslocamentos de disco: imagem por ressonância magnética. **Radiologia Brasileira**, v.37, n.6, p. 449-454, nov. 2004.

SCARF, W.C.; FARMAN, A.G.; SUKOVIC, P. Clinical applications of cone-beam computed tomography in dental practice. **Journal of the Canadian Dental Association,** v.72, n.1, p. 75-80, Feb. 2006.

SCARFE, W.C.; FARMAN, A.G. What is cone-beam ct and how does it work? **The Dental Clinics of North America** v.52, n.4, p. 707-730, Oct. 2008.

SOARES, M.R. et al. Study of effective dose of various protocols in equipment cone beam CT. **Applied Radiation and Isotopes,** v.100, p. 21-26, 2015

SOBOTTA, J. Atlas de anatomia humana sobotta: cabeça, pescoço e extremidade superior. 21 ed. Rio de Janeiro: Guanabara Koogan, 2000.

THERMO ELECTRON CORPORATION. **Model 5500 Automatic TLD Reader with WinREMS^{TM}: Operator's Manual.** Ohio, USA: Radiation Measurement & Protection, 2002.

VOS, W.D.; CASSELMAN, J.; SWENNEN, G.R.J. Cone-beam computerized tomography (CBCT) imaging of the oral and maxillofacial region: A systematic review of the literature. **International Journal of Oral & Maxillofacial Surgery,** v.38, n.6, p. 609-625, June 2009.

WHITE, D.R.; WOODARD, H.Q. Hammond SM. Average soft-tissue and bone models for use in radiation dosimetry. **The British Journal of Radiology**, v.60, n. 1, p. 907-913, 1987.

ZHANG, Z.L. et al. Detection accuracy of condylar bony defects in Promax 3D cone beam CT images scanned with different protocols. **Dentomaxillofacial Radiology,** v.42, n.20120241, p. 1-6, 2013.

ZENÓBIO, E.G. et al. Absorbed radiation doses during tomographic examinations in dental implant planning: a study in humans. **Clinical Implant Dentistry and Related Research,** v.14, n. 3, p. 366-372, 2012.